Copyright Warning & Restrictions

The copyright law of the United States (Title 17, United States Code) governs the making of photocopies or other reproductions of copyrighted material.

Under certain conditions specified in the law, libraries and archives are authorized to furnish a photocopy or other reproduction. One of these specified conditions is that the photocopy or reproduction is not to be "used for any purpose other than private study, scholarship, or research." If a, user makes a request for, or later uses, a photocopy or reproduction for purposes in excess of "fair use" that user may be liable for copyright infringement,

This institution reserves the right to refuse to accept a copying order if, in its judgment, fulfillment of the order would involve violation of copyright law.

Please Note: The author retains the copyright while the New Jersey Institute of Technology reserves the right to distribute this thesis or dissertation

Printing note: If you do not wish to print this page, then select "Pages from: first page # to: last page #" on the print dialog screen

Title of Thesis : An investigation of electrical and optical properties of sputtered amorphous Silicon Nitride and Germanium thin films.

Rajendra S.Khandelwal, Master of Science in Electrical Engineering, 1987

Thesis directed by:Dr. K. S. Sohn, Associate Professor of Electrical Engineering Department.

ABSTRACT

Low temperature preparation of thin amorphous Silicon Nitride and Germanium Films by direct RF sputter deposition was investigated. Influence of various sputtering parameters on film properties was studied. Infrared transmission spectrophotometry was used to evaluate optical properties of the films whereas electrical characteristics of the films were determined from current-voltage measurements of MIS structures. For Silicon Nitride films it was observed that the stoichiometry, as indicated by the IR transmission, dielectric constant and current density versus square root of electric field measurements, was a strong function of the sputtering gas composition and particularly the Ar/N ratio in the sputtering gas. It was established from the current-voltage relationship that the dominant conduction mechanism in these films is of Poole-Frenkel type. The current-voltage characteristics of the

MIS devices were observed to be independent of the electrode material, device area and the film thickness. It is concluded that the insulating films thus deposited were comparable to those deposited using any other deposition method and is anticipated that due to the low deposition temperatures, sputtering may emerge as a highly potential process for optoelectronic device passivation.

Germanium Gamma-ray p-n junction detectors coated with 30 nm thick sputtered amorphous germanium exhibited improved surface stability. Hydrogenated amorphous germanium was also used and the result indicated that this material would have superior passivating properties than amorphous Germanium.

AN INVESTIGATION OF ELECTRICAL AND OPTICAL PROPERTIES OF SPUTTERED AMORPHOUS SILICON NITRIDE AND GERMANIUM THIN FILMS

BY

RAJENDRA S. KHANDELWAL

A THESIS SUBMITTED TO THE FACULTY OF GRADUATE SCHOOL IN PARTIAL FULFILLMENT OF THE REQUIREMENTS FOR THE DEGREE OF
MASTER OF SCIENCE IN ELECTRICAL ENGINEERING
AT
NEW JERSEY INSTITUTE OF TECHNOLOGY
(1987)

APPROVAL SHEET

TITLE OF THESIS: AN INVESTIGATION OF ELECTRICAL AND OPTICAL PROPERTIES OF SPUTTERED AMORPHOUS SILICON-NITRIDE AND GERMANIUM THIN FILMS

NAME AND DEGREE: RAJENDRA S. KHANDELWAL
MASTER OF SCIENCE IN ELECTRICAL ENGINEERING

DEPARTMENT/SCHOOL: ELECTRICAL ENGINEERING
NEW JERSEY INSTITUTE OF TECHNOLOGY
NEWARK, NJ 07102

THESIS AND ABSTRACT APPROVED: _____ _____
DATE

Dr. KENNETH S. SOHN
ASSOCIATE PROFESSOR
DEPARTMENT OF ELECTRICAL ENGINEERING

APPROVAL OF FACULTY COMMITTEE: _____ _____
DATE

Dr. ROY H. CORNELY
PROFESSOR
DEPARTMENT OF ELECTRICAL ENGINEERING

_____ _____
DATE

Dr. WARREN H. BALL
ASSOCIATE CHAIRMAN
DEPARTMENT OF ELECTRICAL ENGINEERING

VITA

NAME OF CANDIDATE : RAJENDRA S. KHANDELWAL

PERMANENT ADDRESS :

DEGREE AND DATE TO BE CONFERRED : MSEE, MAY 1987

DATE OF BIRTH :

PLACE OF BIRTH :

SECONDARY EDUCATION : MARWARI VIDHYALAYA HIGH SCHOOL, INDIA

COLLEGIATE INSTITUTIONS ATTENDED	DATES	DEGREE
M.S.RAMAIAH INST.OF TECH.,INDIA	1978-83	BSEE
NJ INSTITUTE OF TECHNOLOGY, NJ	1984-86	MSEE

MAJOR : ELECTRICAL ENGINEERING

POSITIONS HELD : RESEARCH ASSISTANT 5/85 TO 5/87
DREXLER MICROELECTRONICS LAB, NJIT

ASSISTANT ENGINEER 4/84 TO 9/84
SHANTI ELECTRIC CO. INDIA

ACKNOWLEDGEMENTS

I would like to express my deep gratitude to Dr. Kenneth S. Sohn for his endless cooperation and technical guidance in the preparation of this thesis. His invaluable support and the enthusiastic encouragement provided throughout the course of this research and assistance in furthering my professional talents can not be described by mere words, but comes from my heart that has realized and discovered a highly intellectual personality in such a simple form as he is.

I would like to take this opportunity to express my sincere appreciation and indebtedness to Dr. Roy H. Cornely for developing my interest in semiconductors and for providing constructive criticism and his invaluable time.

I also acknowledge the financial support provided by the State of New Jersey Commission on Science and Technology, Princeton Gamma Tech., Infrared Associates, Inc., and Epitaxx Corp.

Special thanks are due to the members of the Drexler Microelectronics Laboratories for their cooperation.

I would like to thank Mr. Sudheer Solapurkar for formatting the graphs and tables.

CONTENTS

APPENDICES

LIST OF FIGURES

LIST OF TABLES

I INTRODUCTION

Research reported in this thesis is based upon the experiments conducted in order to carry out a research project on passivation of semiconductor surfaces, under the supervision of Dr. K. Sohn and Dr. R. H. Cornely at Drexler Microelectronics Laboratories, N.J.I.T., funded by The State of New Jersey Commission on Science and Technology. Several industries also participated actively in this research. The primary goals of this research were to prepare and characterize the passivating coatings of Silicon Nitride and Germanium for Opto-electronic devices. Passivating coatings are of significant importance for device performance. They are essential for a device in order to protect its characteristics from deteriorating due to environmental hazards like diffusion of moisture and other impurities.

These coatings were to be deposited by Sputter Technology, where low deposition temperature is the most attractive feature from the point of view of passivation of III-V compound devices, over CVD; a more widely accepted technology for Silicon Nitride deposition. Various researchers have reported successfully prepared Silicon Nitride films obtained by CVD.[23,27] The main disadvantage

of CVD is the high deposition temperature required from the point of view of passivation of III-V devices. To keep up with the continuing technical advancement, there has always been felt a need for better deposition process.

Direct RF sputtering of Silicon nitride target (hot pressed powder target) has been avoided because of difficulties encountered in obtaining high purity targets.[37] Various difficulties experienced have been reported by several researchers.[38,39,40,43] This research is an attempt to resolve some of these difficulties and to study the films thus prepared.

An attempt was made to prepare thin insulating films of Si_3N_4 by direct RF sputtering of Silicon Nitride target. Sputtering parameters were varied and a study of effects of these parameters on the growth behavior of the films was conducted. The effect of sputtering medium on film quality and its electrical characteristics was also studied using IR spectrophotometry and I-V measurements. It was concluded that reasonably good insulating films of Si_3N_4 can be prepared by direct RF sputtering in the Nitrogen ambient.

Thin films of amorphous Germanium were also prepared by direct RF sputtering of Germanium target. Ge, although an established semiconductor, exhibits dielectric properties in its amorphous state. Quite encouraging

results were obtained. Amorphous Germanium has attracted a great deal of attention recently and is anticipated that it might assume a significant role in semiconductor industry, as a passivating material.

Apart from the preperation and characterization of Si_3N_4 and a-Ge thin films, a great deal of time was spent on decontamination and modification of the sputtering system.

Experimental procedure, film characterization, results and discussions are further explained in detail in the various sections of this report. Following is a brief overview of each chapter of this thesis.

Questions like What is surface passivation? and Why do we need it? are answered in chapter II. Various passivating materials and deposition processes are compared. Characterization techniques for these films are also discussed.

A theoretical review of conduction mechanisms in thin insulating films is discussed in chapter III. Various mechanisms are introduced and Poole-Frenkel effect is discussed in detail. Further, it also highlights the complications involved in the study of conduction processes in thin film insulators.

Various facilities available and measurement techniques employed by the author to characterize the

insulating films studied in this research are introduced in chapter IV.

Chapter V details the experimental procedure and precautionary measures required to obtain good quality films. Operation of the sputtering system is also explained and it is hoped that the information provided in this chapter will be of immense help to new graduate students wishing to participate in thin film research at this laboratory.

Experimental data and results obtained are presented in chapter VI. Sample calculations are also shown in this chapter.

A comprehensive discussion of results of this research is presented in chapter VII. Influence of variations in sputtering parameters on growth process, electrical properties, and optical transmission are discussed.

Finally, concluding remarks and suggestions for future work are presented in chapter VIII.

II PASSIVATION OF SEMICONDUCTOR SURFACES

2.1.0 INTRODUCTION:

Semiconductor surface properties differ very much from bulk properties, and these surface properties can influence the device performance significantly. Figure 2.1 illustrates one facet of this influence. The space charge layer separating the two regions of the junction has to reach the surface and there its width is largely determined by the nature of the surface charges, the defect centers there contribute the leakage current. These surface properties can dominate the desired electrical characteristics of the junction, which is undesirable, since surface dominated characteristics are usually less stable than the bulk dominated characteristics. Furthermore, surface properties are markedly affected by the small amounts of contaminants picked up during processing and thence the device characteristics can change in an uncontrolled manner.

On real surfaces, the density and distribution of surface states are altered by the absorbed species, structural defects and impurities. One particular case of interest is the interface formed by the intimate contact of semiconductor surface with another solid phase such as an oxide layer. Most of the surface states are used by the

oxide layer through bond formation and as a result, the number of surface states actually observed is several orders of magnitude smaller than that expected by theory for an ideal surface, which is of the order of the number of surface atoms. The residual non bonding electron at the surface is often termed as Dangling Bond. Now, presence of charge in an oxide layer on the surface of a crystal can develop Surface Potential (χ_s) at the interface.

For a semiconductor, effects of surface potential are observed to a great extent since the charge density is much lower. The affected region near the surface is called Space Charge Region, and is a complex function of surface potential, carrier density, and the time dependent behavior of the oxide-semiconductor surface. This effect is illustrated in the energy band diagram shown in Figure 2.2.

With this background, meaning of the term **"Passivation"** will be explained and defined. Chemically speaking, passivation refers to the process of rendering a surface nonreactive. In case of semiconductors, both chemical as well as electrical stability is required in a passivated surface. Hence from semiconductor point of view, surface passivation implies both chemical as well as electrical stabilization. In other words, semiconductor surface passivation minimizes the semiconductor surface contribution towards the electrical properties of the

device. It is accomplished by depositing a thin insulating layer (film) on the semiconductor surface to be passivated.

2.2.0 TYPES OF PASSIVATING COATINGS:

Broadly speaking, passivation coatings can be classified in two major categories:

(i) PRIMARY PASSIVATION: It refers to the film which is directly in contact with the substrate from which device is to be fabricated. Their main objectives are control and stabilization of the semiconductor surface electrical properties, which include good dielectric properties, low surface recombination velocity, controlled immobile charge density, device stability at elevated temperatures under bias or operating conditions etc.

(ii) SECONDARY PASSIVATION: It refers to the passivation coating used for the protection and stabilization of the primary passivation. This implies that they are separated from the substrate, from which the device is to be fabricated, by an underlying dielectric layer. It serves the function of insulating and protecting the interconnections and metallization, overall mechanical and chemical protection.

2.3.0 REQUIREMENTS OF PASSIVATING COATINGS:

The electrical requirements of an ideal passivating layer may be summarized as follows:

(i) The semiconductor surface potential must not change significantly with time under the stress conditions encountered by the device.

(ii) The semiconductor surface potential should be optimum for the particular device.

(iii) Device requirement of surface state density and the surface charge shall be met by the passivation.

2.4.0 SEQUENCE OF APPLICATION OF PASSIVATING LAYERS:

Passivation coatings may be applied before or after the metallization. Sequence of application of passivation layers to various types of Silicon devices is shown in the self-explanatory Figure 2.3.

2.5.0 CHARACTERIZATION OF PASSIVATING FILMS:

Passivating films used in semiconductor applications are characterized by standard chemical, physical and electrical methods established for surface and thin film analysis and by the methods developed specifically for analysis of thin insulating films. One of the most widely employed electrical methods is the

determination of Capacitance-Voltage (C-V) relationship of Metal-Insulator-Semiconductor structure, before and after bias-heat treatment. From these electrical measurements one can calculate the density of electronic states, interface charges and bulk charges, all of which play important roles in the electrical properties and stability of deposited films.[1,2,3,4] X-ray Fluorescence analysis,[5,6,7] Backscattering and Auger Electron Spectroscopy (AES)[8] have been used to determine the composition of the deposited dielectric film. Infrared Spectroscopy has been used extensively for compositional, structural and optical absorption analysis of the deposited dielectric films. Moisture absorption and adsorption, and resistance of deposited dielectric films to moisture have been reported in literature.[9,10,11] Measurement of surface conductivity,[12] stress[13,14,15] and index of refraction[16,17,18] of various dielectrics have been reported. Chemical etch rate measurements have been used to determine the film composition and relative density.[16,17,19]

2.6.0 COMPARISON OF VARIOUS PASSIVATING MATERIALS AND DEPOSITION PROCESSES:

2.6.1 OXIDES:

Improvement in the device performance due to

thermally grown Silicon dioxide (SiO_2) was first reported by Atalla et al.[20] Passivating film properties which have major effects on device performance and stability are following:

(1) Dielectric breakdown strength.

(2) Interface state density.

(3) Fixed charges.

(4) Drift.

Oxides were considered extremely useful and beneficial coatings from the point of view of processing simply because of the fact that Silicon has a native oxide layer of approximately 5 nm. There are several methods used for the deposition of SiO_2 thin films such as plasma anodization, wet anodization, thermal oxidation, chemical vapor deposition (CVD), RF sputtering etc. to list a few of them.

The most commonly used primary passivation material is thermally grown SiO_2 (0.5-1.5 micron). In addition to thermally grown oxides, oxides are also prepared by high temperature oxidation, at atmospheric pressure, of Si wafer in atmosphere of dry Oxygen, wet Oxygen or steam. RF sputtered SiO_2 films have been observed to have good coverage of topography and low compressive stress, but at the same time sputtering can produce radiation damage in thermally grown SiO_2. Properties of

SiO_2 deposited using different methods are compared in Table 2.1.

Layers of Phosphosilicate glass (PSG) have been widely used because they are having less tensile stress than SiO_2 as deposited by CVD, and have better ability to getter alkali ions.

CVD has been used more widely than RF sputtering for depositing SiO_2, PSG, BSG etc. because it is faster, requires simpler equipment, and in contrast to RF sputtering, it produces no radiation damage in the thermally grown SiO_2.

2.6.2 SILICON NITRIDE (Si_3N_4) AS A PASSIVATING MATERIAL:

Silicon Nitride is considered as an important material for passivation since it is one of the best barriers to the migration of ions and water and can also serve as an oxidation mask in making self aligned device structures. In general, it serves as both a getter as well as an effective alkali barrier. It has been widely studied as a possible insulator in MIS structures since it is more resistant to radiation, and because of the above mentioned properties. As compared to SiO_2, Si_3N_4 has higher dielectric constant. A comparison of various properties of SiO_2 and Si_3N_4 deposited using different techniques is given in Table 2.2. Properties of plasma and LPCVD Nitrides

are compared in Table 2.3.

Silicon Nitride is also considered to be a very important material for the passivation of opto-electronic devices, since native oxides that forms on the surface of III-V materials are not as chemically stable as the native oxide on Silicon. Inorganic materials for passivation of III-V compounds are usually deposited using glow discharge (plasma assisted) deposition. One of the most critical factors that determines the deposition process for passivation of opto-electronic devices is the deposition temperature. The deposition of passivating material has to be performed at relatively low temperature ($< 400^{o}$ C) to avoid decomposition of the semiconducting compounds. These devices usually employ Arsenic, Phosphorous, Indium etc., all of which vaporise at relatively low temperatures. Sputtering offers low deposition temperatures as compared to CVD and thus it was selected as a deposition process for this research. Considering the potential of Silicon Nitride as a passivant for both Si as well as III-V compounds, it was decided to study this material.

2.6.3 AMORPHOUS GERMANIUM (a-Ge) AS A PASSIVATING MATERIAL:

Application of Germanium in semiconductor devices has always been avoided mainly due to the lack of a stable, passivating native oxide. However, for certain special

applications like nuclear radiation detectors, one still finds Ge as an indispensible semiconductor. If Ge nuclear detectors are to be stabalized, the surface passivation must be done in order to produce flat band condition. Only passivant used for Ge detectors is SiO, which is found to be unsatisfactory for the following reasons:[35]

(1) The surface compensation is sensitive to the initial state of the surface.

(2) The surface compensation is not adjustable to F.B. condition.

(3) The passivated devices have a higher leakage current.

(4) An additional 1/f noise is often introduced.

(5) The method of application (thermal evaporation) limits the application to simple geometries only.

Experimental studies were carried out on various passivating materials to avoid the above mentioned detrimental effects of SiO. It appears that sputtered hydrogenated amorphous Ge (a-Ge:H) may be a better choice. Figure 2.4 compares the effect of SiO and a-Ge:H on detector leakage current as a function of temperature. It can be inferred from this plot that a-Ge:H is a better substitute for SiO.

The ability to make passivated surfaces with flat band condition on Ge nuclear detectors can extend the application of these as well other Ge devices.

Thus with the objective of making Ge a more useful semiconductor, research on semiconductor surface passivation was extended to Germanium.

2.6.4 APPLICATIONS OF SPUTTERED a-Ge:H FILMS:

An important application of this technique is in making multi-detector arrays for which case detector can be fabricated and tested one-by-one without concern for any ambient degradation before mounting in the final system. Another important application will be for charged-particle telescope where the freedom from entrance windows will allow the fabrication of detectors many centimeters deep using normal thick Lithium contacts. The fact that a-Ge coating more than 1 um thick are opaque to visible light will allow detectors to be operated in conditions where such light can not be avoided.

Another important property of the a-Ge:H passivation is that it is unaffected by rather high temperature ($300^{o}C$) anneals. Thus radiation damaged detectors can be thoroughly annealed without any intermediate chemical treatment.

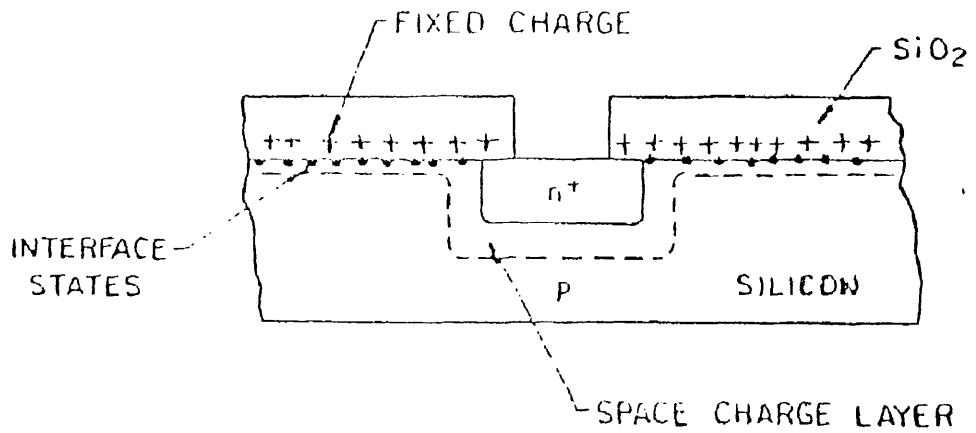

Fig. 2.1 CROSS SECTION OF P-N JUNCTION STRUCTURE IN THERMAL EQUILIBIRIUM SHOWING POSITIVE FIXED CHARGE AND INTERFACE STATES AT Si-SiO_2 INTERFACE. FIXED CHARGE AND CHARGED INTERFACE STATES ARE ASSUMED LARGE ENOUGH TO CAUSE THE SPACE CHARGE LAYER TO EXTEND ALONG THE SILICON SURFACE BEYOND THE JUNCTION.

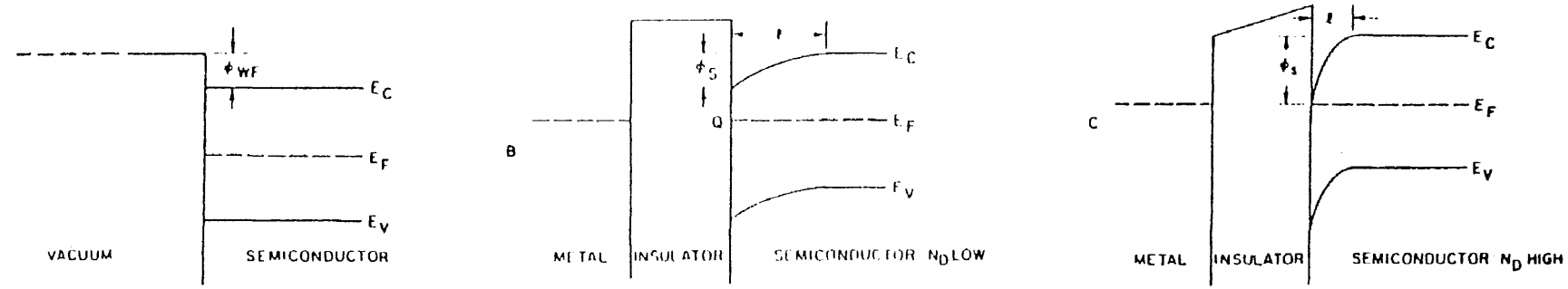

Fig. 2.2 *Energy-band diagrams (one-dimensional). (A) Free semiconductor surface in vacuum with no surface charge. φ_{WF} is the work function; (B) Metal-insulator-semiconductor system showing surface potential φ_s over distance t for low doping level N_D caused by charge Q; (C) Metal-insulator-semiconductor system showing φ_s over shorter distance t (N_D high) and onset of inversion (large φ_s) due to applied voltage on metal.*

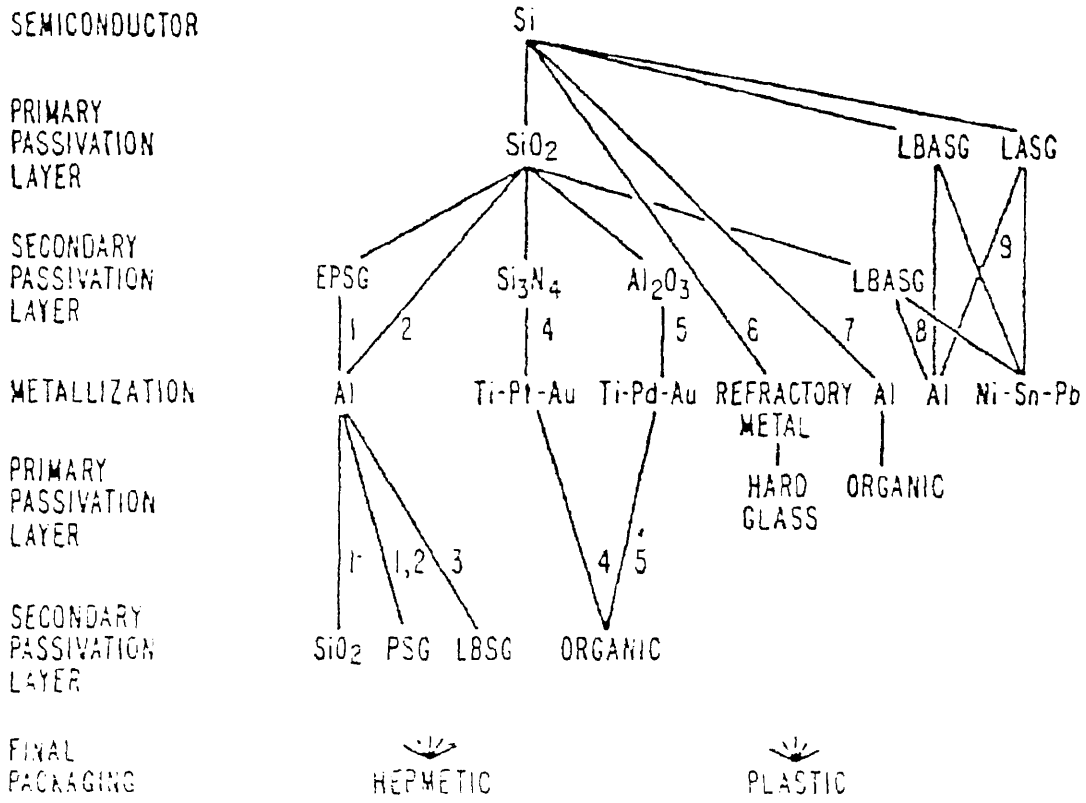

Fig. 2.3 Sequence of application of passivation layers to various types of silicon devices. Typical devices made by the sequences indicated by numbers are as follows: 1, NPN transistors, digital and linear bipolar IC's; 2, MOS transistors, p-channel MOS IC's, CMOS; 3, face-bonded chips; 4, beam-lead sealed-junction bipolar devices, plastic encapsulated Au-metallized devices; 5, beam-lead sealed-junction MOS IC's; 6, axial-lead diodes; 7, high-power diodes, high-power transistors, thyristors, devices with beveled junction; 8, high-voltage devices, high-voltage power devices; 9, high-voltage devices. Designations for glasses are as follows: EPSG, phosphosilicate glass formed by NPN bipolar transistor emitter diffusion; LASG, lead aluminosilicate glass; LBASG, lead boroaluminosilicate glass; LBSG, lead borosilicate glass; PSG, phosphosilicate glass.

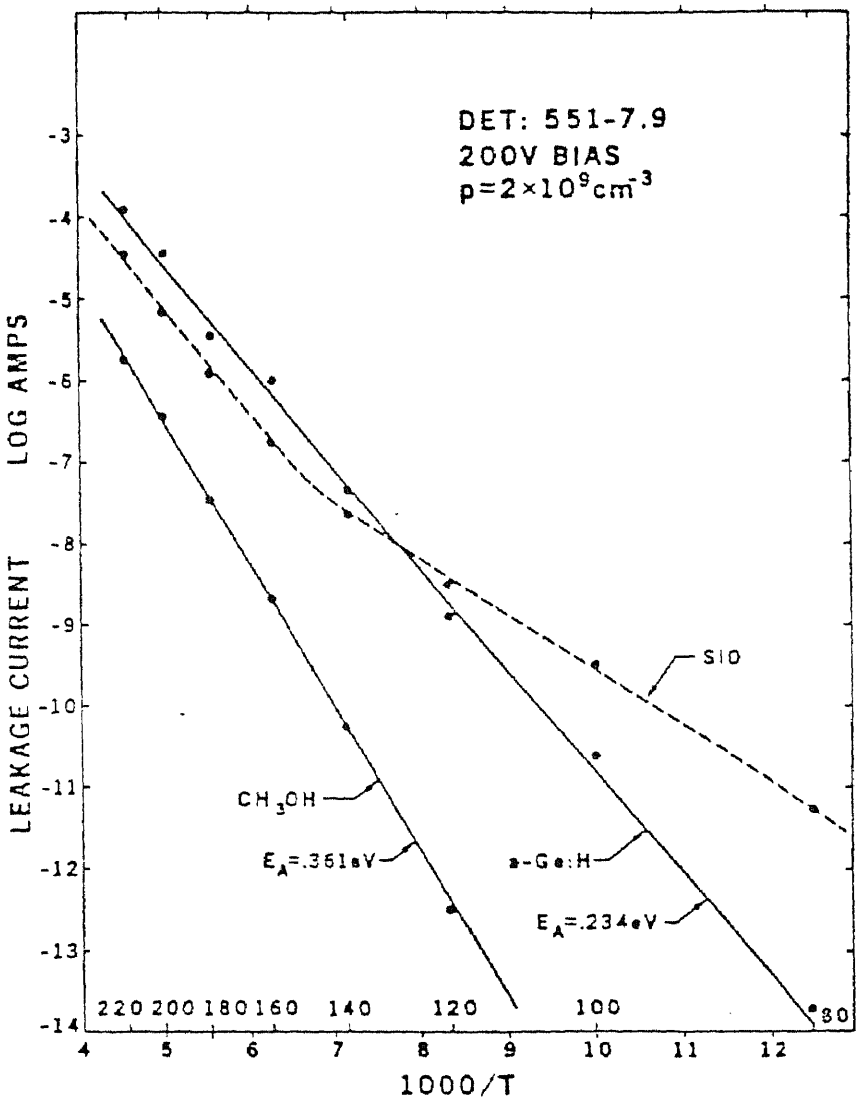

Fig. 2.4 Detector leakage current as a function of temperature for bare, a-Ge:H and SiO coated surfaces.

Table 2.1

Properties of Deposited Silicon Dioxide.

Deposition	Plasma	$SiH_4 + O_2$	TEOS	$SiCl_2H_2 + N_2O$
Temperature °C	200	450	700	900
Composition	$SiO_{1.9}(H)$	$SiO_2(H)$	SiO_2	$SiO_2(Cl)$
Step Coverage	nonconformal	nonconformal	conformal	conformal
Thermal Stability	looses H	densifies	stable	looses Cl
Density g/cm^3	2.3	2.1	2.2	2.2
Refractive Index	1.47	1.44	1.46	1.46
Stress 10^9 dyn/cm^2	3 C-3 T	3 T	1 C	3 C
Dielectric Strength 10^6 V/cm	3-6	8	10	10
Etch Rate, Å/min (100:1 H_2O:HF)	400	60	30	30

Table 2.2

COMPARISON OF DIELECTRIC FILMS

	SILICON DIOXIDE			SILICON NITRIDE	
DEPOSITION	PLASMA	SiH_4+O_2	TEOS	PLASMA	SiH_4+NH_3
TEMPERATURE, °C	200	450	700	350	700
COMPOSITION	$SiO_{1.9}$ (H)	SiO_2(H)	SiO_2	SiN_xH_y	Si_3N_4 (H)
ATOM % H	5-10	2-4	<1	20-25	4-8
REFRACTIVE INDEX	1.47	1.44	1.46	2.0-2.2	2.01
DENSITY, g/cm^3	2.3	2.1	2.2	2.4-2.8	3.0
STRESS, 10^9 dyn/cm^2	3C-3T	3T	1C	2C-5T	10T
DIELECTRIC STRENGTH 10^6 V/cm	3-6	8	10	3-6	10
RESISTIVITY, Ω−cm	10^{13}–10^{14}	10^{15}	10^{16}	10^{12}–10^{15}	10^{16}
STEP COVERAGE	Poor	Poor	Conformal	Poor	Conformal
THERMAL STABILITY	Looses H	Densifies	Stable	Cracks	Stable

Table 2.3

Properties of Silicon Nitride

Deposition	LPCVD	Plasma
Temperature °C	700-800	250-350
Composition	$Si_3N_4(H)$	SiN_xH_y
Si/N Ratio	0.75	0.8-1.2
Atom % H	4-8	20-30
Refractive Index	2.01	1.9-2.2
Density g/cm^3	2.9-3.1	2.4-2.8
Dielectric Constant	6-7	6-9
Resistivity Ω-cm	10^{16}	10^6-10^{15}
Dielectric Strength 10^6 V/cm	10	5
Energy Gap eV	5	3-4
Stress 10^9 dyn/cm^2	1 T	2 C-5 T

III CONDUCTION MECHANISMS IN THIN INSULATING FILMS

3.1.0 INTRODUCTION:

A brief review of various conduction mechanisms in thin insulating films will be discussed in this chapter. Although, it is out of the scope to discuss all the mechanisms in detail, an attempt is made to present an introduction and for those interested in details, a number of references are listed. Since we are concerned with thin films, it is apparent that we will be concerned mainly with the high field electrical properties of these films, since as low as even a few volts will induce fields of the order of 10^4-10^5 v/cm in the films. High field electrical properties can not be adequately described by a single conduction process; usually the various field strength ranges manifest different electrical phenomena.

3.2.0 CONDUCTIVITY OF THIN FILMS:

An insulator is a material which contains very few volume-generated carriers (<1 per cm^3), and thus has virtually no conductivity. Electrical properties of thin film insulators are determined not by intrinsic properties of the insulators but by the other properties, such as the nature of the electrode insulator contact. A suitable

(ohmic) contact is capable of injecting additional carriers into the insulator, far in excess of the bulk generated carriers. Further, as mentioned above, very high fields can be generated in a thin film insulator at the cathode-insulator interface simply by the application of a very low bias (of the order of a few volts). For fields in excess of 10^6 v/cm, field-emission injection of relatively large currents from the cathode into the conduction band of the insulator is possible.

There are several reasons for believing that the observed conductivity in thin film insulators is often due to extrinsically rather than intrinsically bulk generated carriers.

consider the intrinsic current density carried by an insulator

$$J = e \mu N_c \exp [-E_g/2kT] \quad \text{---------(3.1)}$$

where e = Electronic charge = $1.6*10^{-19}$ C,

μ = Mobility (cm^2/v-sec),

N_c = Effective density of states in an insulator (cm^{-3}),

E_g = Insulator band gap energy (eV),

k = Boltzmann constant = $8.6*10^{-5}$ eV,

T = Absolute temperature (^oK).

Using this expression, current densities obtained are many orders of magnitude smaller than the actual

current densities observed.[28] Further observed thermal activation energy associated with conductivity of the films is much smaller than would be expected (~ $E_g/2$), if the conductivity were intrinsic in nature.

Source of extrinsic conductivity is thought to be the inherent defect nature of the films. Stoichiometric films of the composed insulators are notoreously difficult to prepare, for the reasons discussed in this thesis. For example, SiO yields a film containing a mixture of compounds varying from SiO to SiO_2, as well as free Si.[29,30,31] Free Si may act as donor centers in these films.[32] A further problem arises due to the contamination incorporated in vacuum deposited films.

It has been postulated that the insulator contains very high donor density.[28] At low temperatures, very few donors are ionized, i.e., there are very few carriers in the conduction band of insulator. Thus the bulk has a high resistivity.

Another important fact to be considered in thin film insulators is traps. Insulating films are usually amorphous or polycrystalline. For crystalline size of 10 nm, trapping levels as high as 10^{18} are possible because of grain boundary defect only. Furthermore, vacuum deposited films contain large stresses which induce further trapping centers.

Thus it is believed that vacuum deposited films contain a large density of both impurity and trapping centers, and judicious study of electrical conduction in such films can not be accomplished without due consideration of these possibilities.

For insulators with large energy gaps (E_g > 3 eV), electronic conduction is supposed to be dominated over hole conduction according to the following explanation. The hole mobility is usually much lower than the electron mobility and thus the hole contribution to the conductivity can usually be neglected. Also, in practical insulating films, as mentioned earlier, the trapping density is high, the tendency is for a free hole to be trapped quickly and thus become immobilized.

3.3.0 BAND THEORY OF INSULATORS:

According to Pauli principle, each energy band of a crystal, consisting of N atoms, has space for 2N electrons per atom. If the highest filled band of a crystal is occupied by two electrons per atom, i.e., if the band is completely filled, we would expect that the electrons can not drift through the crystal when an external electric field is applied (similarly as it is impossible to move a car in a completely occupied parking lot). An electron has to absorb energy in order to move. Keeping in mind that for

a completely occupied band, higher energy levels are not allowed. (Possibility of electron jumping to a higher band is excluded.) Solids in which the highest filled band is completely occupied by electrons, are therefore, Insulators. The energy band diagram for an insulator is shown in Figure 3.1.

3.4.0 CONDUCTION MECHANISMS IN DIELECTRIC FILMS:

There are several mechanisms associated with the electronic conduction in thin dielectric films and a brief introduction is given here. However, it is not possible to discuss all the mechanisms in detail, only those related to this work are given more attention. For a given insulator, each conduction process may dominate in certain temperature and voltage range and the processes are not exactly independent of one another, which increases complexity in study of these mechanisms.

Table 3.1 summarizes the basic conduction processes in insulators. Schottky emission is one in which conduction is due to thermionic emission across the metal-insulator interface or the insulator-semiconductor interface. Poole-Frenkel[33] emission is due to field-enhanced thermal excitation of trapped electrons into the conduction band. these two mechanisms are discussed in the section 3.5.0. The tunnel emission is caused by field

ionization of trapped electrons into the conduction band. Further, electrons tunneling from the metal Fermi energy into the insulator conduction band also contribute towards the tunnel emission. however, the tunneling occurs only in ultrathin films or at very high fields. From the table 3.1, one can say that the tunnel emission has strongest dependence on the applied voltage but is essentially independent of temperature. The space-charge-limited current results from a carrier injected into the insulator, where no compensating charge is present and is also independent of temperature. Ohmic current is carried by thermally excited electrons hopping from one isolated state to the next. It is exponentially dependent on temperature. For further details, reader may refer to the references listed[28,44] at the end.

3.5.0 POOLE-FRENKEL EFFECT:

Poole-Frankel effect has been quite frequently invoked in the interpretation of the electric current in the dielectric films at high electric fields (> 10^4 v/cm). This effect is analogous to the Schottky effect for a plain electrode: a lowering of potential barrier V_g sorrounding a localized charge under the influence of an external electric field. The Schottky effect is thermionic emission over a field-lowered barrier (Figure 3.2), and the

expression is usually written in the form

$$I = I_o \exp [e(B_S E^{1/2} - V_g)/kT] \quad \text{------(4.2)}$$

where the Schottky field-lowering coefficient B_S is given by

$$B_S = (e/4\pi\epsilon_o\epsilon_r)^{1/2}$$

where ϵ_o = Permittivity of free space,

ϵ_r = Dielectric constant.

Now, in case of a point defect sorrounded by Coulombic potential, as may be the case, for example, with a donor-like centre in a crystalline lattice, the Poole-Frenkel effect is obtained.[33] It can be defined as the lowering of a Coulombic potential barrier when it interacts with an electric field. Field lowering of the barrier height is now given by $B_{PF}E^{1/2}$, where the Poole-Frenkel coefficient $B_{PF} = 2B_S$ (Figure 3.3). Barrier height is the depth of the trap potential well and factor of two comes from the fact that the barrier lowering is twice as large due to the immobility of the positive charge.

Further comments on Poole-Frenkel effect will be made in the discussion of results of this research, where a comparison of results obtained by several other researchers is presented.

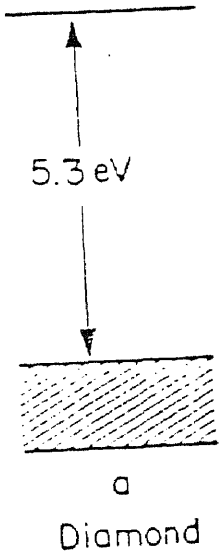

Fig. 3.1 BAND-DIAGRAM OF AN INSULATOR

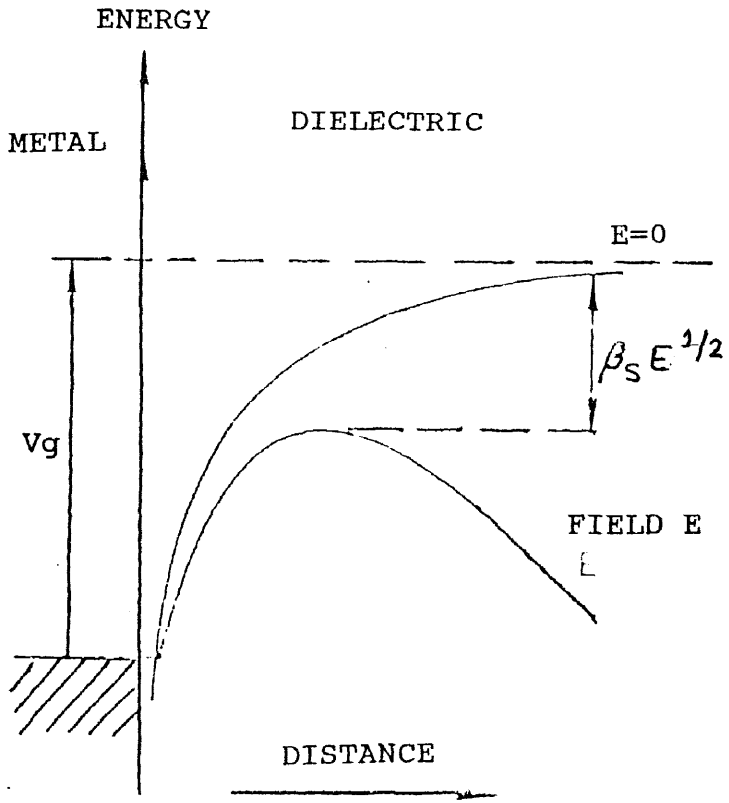

Fig. 3.2 THE SCHOTTKY EFFECT WITH A PLANAR CATHODE.

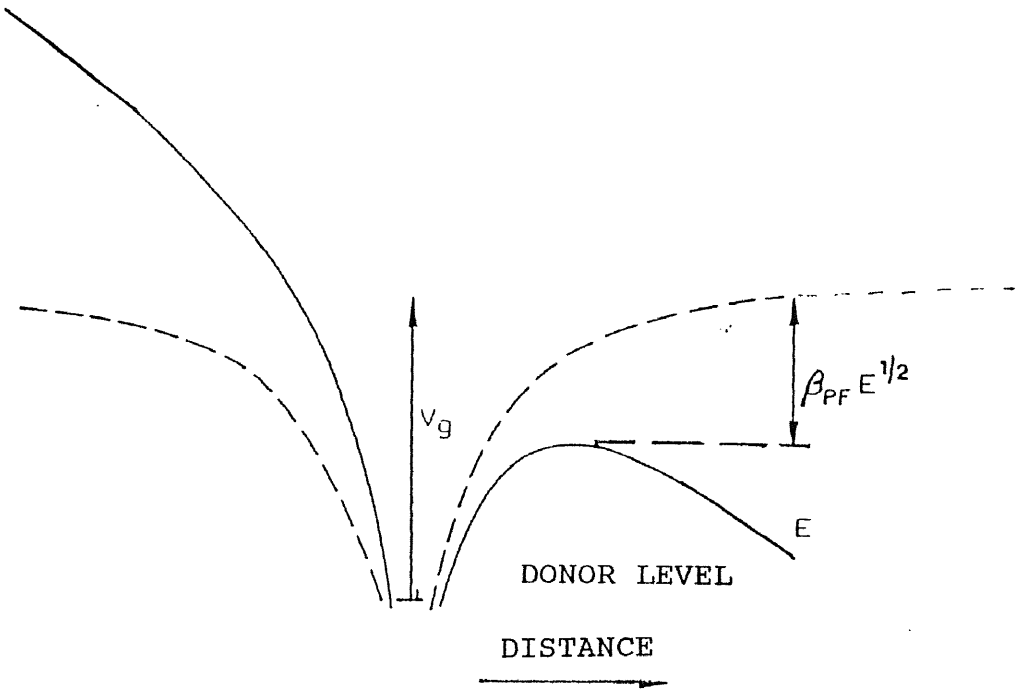

Fig. 3.3 POOLE-FRENKEL EFFECT FOR ELECTRON EMISSION FROM A POINT DEFECT

Table 3.1 Basic Conduction Processes in Insulators

Process	Expression[a]	Voltage and Temperature Dependence[b]
Schottky emission	$J = A^* T^2 \exp\left[\frac{-q(\phi_B - \sqrt{q\mathcal{E}/4\pi\epsilon_i})}{kT}\right]$	$\sim T^2 \exp(+a\sqrt{V}/T - q\phi_B/kT)$
Frenkel–Poole emission	$J \sim \mathcal{E} \exp\left[\frac{-q(\phi_B - \sqrt{q\mathcal{E}/\pi\epsilon_i})}{kT}\right]$	$\sim V \exp(+2a\sqrt{V}/T - q\phi_B/kT)$
Tunnel or field emission	$J \sim \mathcal{E}^2 \exp\left[-\frac{4\sqrt{2m^*}(q\phi_B)^{3/2}}{3qh\mathcal{E}}\right]$	$\sim V^2 \exp(-b/V)$
Space-charge-limited	$J = \frac{8\epsilon_i \mu V^2}{9d^3}$	$\sim V^2$
Ohmic	$J \sim \mathcal{E} \exp(-\Delta E_{ae}/kT)$	$\sim V \exp(-c/T)$
Ionic conduction	$J \sim \frac{\mathcal{E}}{T} \exp(-\Delta E_{ai}/kT)$	$\sim \frac{V}{T} \exp(-d'/T)$

[a] A^* = effective Richardson constant, ϕ_B = barrier height, $\mathcal{E}$ = electric field, ϵ_i = insulator dynamic permittivity, m^* = effective mass, d = insulator thickness, ΔE_{ae} = activation energy of electrons, ΔE_{ai} = activation energy of ions, and $a \equiv \sqrt{q/(4\pi\epsilon_i d)}$.
[b] $V = \mathcal{E}d$. Positive constants independent of V or T are b, c, and d'.

IV FILM CHARACTERIZATION

4.1.0 INTRODUCTION:

As described in chapter II, there are a number of ways available for characterization of thin insulating films as far as physical and chemical characterization is concerned, but for electrical characterization, very few methods are available. Most versatile and easily available are Current-Voltage (I-V) and Capacitance-Voltage (C-V) measurement methods. Results of this research are basically based upon optical (Infrared Transmission) and I-V measurements. The measurement techniques are described in this chapter. It is appropriate to remark at this stage that the facilities available in the laboratory at the present time are insufficient for perfect characterization of thin Silicon Nitride insulating films.

4.2.0 THICKNESS MEASUREMENT:

Film thickness had been measured by an Angstrometer (Sloan M-100). This equipment works on the principle of interferrometry and uses a Sodium vapor lamp. Thickness was calculated by using the formula

$$\text{Thickness } (d) = [a/b]*[X/2] \qquad \text{-----(4.1)}$$

where X is the wavelength of Sodium vapor lamp and

X/2 = 294.5 nm,

'a' and 'b' are the distances between the consecutive fringes measured on the angstrometer (Figure 4.1).

To employ this method, it is necessary to create a step on the film whose thickness is to be measured.

4.3.0 X-RAY DIFFRACTION:

X-ray diffraction had been employed to determine the nature of the films and this measurement had confirmed that the films were amorphous. The equipment used for this measurement was General Electric model # GE11GN1 X-ray Diffractometer.

4.4.0 OPTICAL MEASUREMENTS:

Infrared absorption/transmission (IR) measurement is of great importance in determining the quality and composition of thin films. Perkin-Elmer model # 457 Infrared spectrophotometer (dual beam) was used for the measurements. This was very sensitive measurement that determined the state of the films. Alteration in sputtering conditions and parameters for the succeeding experiment were based upon the IR results of the preceeding experiment. It had been observed that for good films IR absorption peak had ocurred at ~ 11.5 to 12 microns. Two samples are required for this measurement. One of the

sample is optical reference sample which is prepared by chemical etching of the Si substrate and the other one is the sample with the Si_3N_4 film. (Both of these samples are from the same Si wafer.) Procedure for the IR measurement is described in the appendix C.

The sample used for optical referance was of the same specifications as that of the actual sample with the Nitride film. Not only did the optical referance attenuate the referance beam to permit the transmittance of highly absorbing Si_3N_4 film but it also cancelled the effect of the filmed sample substrate absorption. The resultant data therefore represented the transmittance through the Silicon Nitride film only.

4.5.0 CAPACITANCE MEASUREMENT:

MIS Capacitors were used for this measurement. In fact this was used for the calculation of the dielectric constant. HP 4261A L-C-R bridge was used for capacitance measurement at 1 Khz and 120 hz. Dielectric Constant was calculated as explained in chapter section 6.3.2.

4.6.0 CURRENT-VOLTAGE (I-V) MEASUREMENTS:

This was very important measurement and this research has basically concentrated on this result. A special assembly was made for holding the samples. Keithley

616 digital electrometer was used for measuring the current and HP 3435A digital multimeter was used for the voltage drop measurements. Circuit diagram is shown in Figure 4.2. Results and interpretetion are discussed in detail in chapter VI and VII.

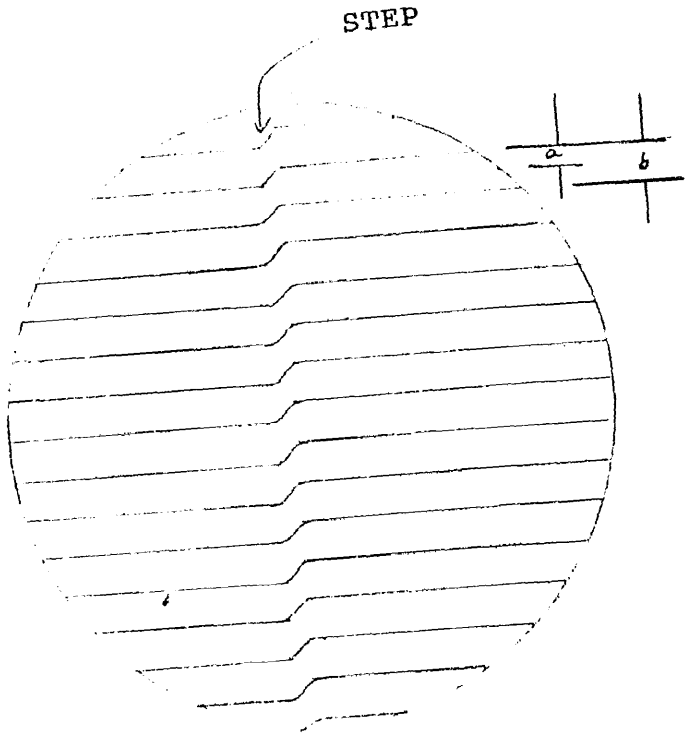

Fig. 4.1 STEP FOR THICKNESS MEASUREMENT.

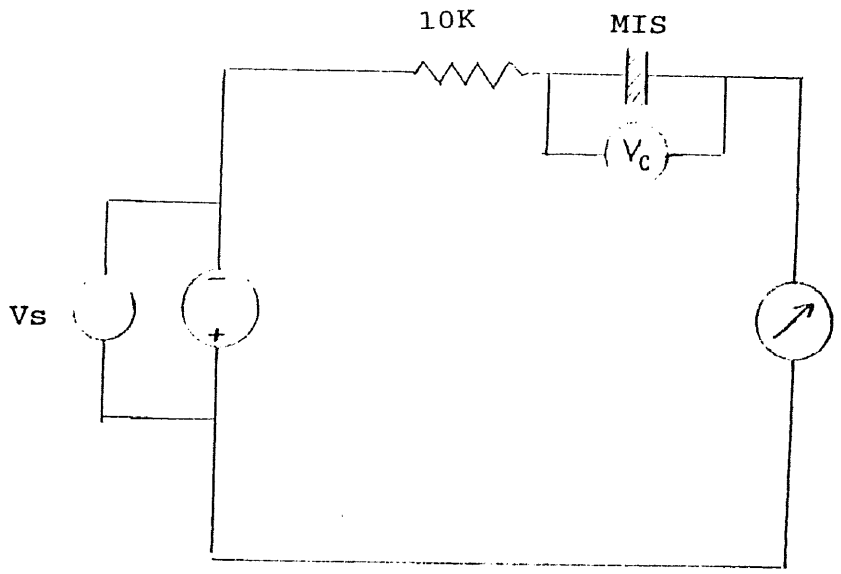

Fig. 4.2 CIRCUIT DIAGRAM FOR I-V MEASUREMENTS.

V EXPERIMENTAL PROCEDURE

5.1.0 MRC 8800 SPUTTERING SYSTEM: AN INTRODUCTION

A modified version of MRC 8800 Sputtering System was used for the deposition of Silicon Nitride thin films. The method of sputtering involved Radio Frequency (RF) sputtering in diode/triode and biased triode modes of operation. Biased sputtering was also carried out in diode mode. biased sputtering improves adhesion and reduces contaminants in the deposited films.

The diode mode was carried out without the plasma confinement box while the plasma confinement box was used in the triode mode. The plasma confinement box (triode box) is a split four part construction so that two central parts are at floating potential with respect to the plasma and therefore do not sputter. This split construction also helps in preventing contamination. This insulated stainless box guides an electron beam perpendicular to the ion motion. A filament supplied with approximately 60 Amps emits the electrons(by thermionic emission) to enhance the ionization of the sputtering gas (Ar^+), allowing sputtering to occur at lower pressure, which increases the mean free path of the sputtered species. The electron flow (I_{DC}) is collected by a dc biased filament at the opposite end of the triode box.

A schematic representation is of the sputtering system is illustrated in Figure 5.1. The rotating target head can accomodate four targets fitted with ground shields. The substrates laid on the movable anode can be heated to the desired temperature by a resistive heating element through the anode and substrate cooling can be achieved using the cooling lines through the anode. However, during this research, substrate temperature was not raised intentionally.

The substrates are laid on the Copper platen in the intervac chamber and then, are transported into the main chamber without breaking vacuum in the main chamber.

Stainless steel construction was preferred for the vacuum chamber because it absorbs relatively much less gassess as compared to other materials like glass, Aluminium etc. Thus prolonged degassing of the chamber is not required. Furthermore, initially it was to be used for the HgCdTe deposition and its essential requirement was to withstand the corrosive Hg atmosphere.

The RF generator is a "Henry 2000" that operates at 13.56 MHz. The Ar gas pressure is monitored using a ionization gauge (Phillips 224). The Ar^+ ion bombardment is essential to eject the atoms (sputtered species) from the multicomponent target (Si_3N_4) material. The gas (Ar) used for sputtering is supplied to the system through a gas

cylinder via a micrometering valve provided on the system.

The most important parameter of the sputtering process (or any other vacuum deposition process) is the vacuum pressure, which using a cryopump (CTI CRYOTORR 8) and 50 mtorr roughing pressure (attained with the mechanical pump), must be below the low 10^{-6} torr range, to consider the vacuum low enough for sputtering. Also, the rise time (t_r) is a very important criterion for good vacuum. This is defined as the time required for the pressure to rise to $5*10^{-5}$ torr with the high vac valve closed and it must be (at least) equal to 60 seconds. To evaluate the importance of low pressure in a vacuum system, Table 5.1 shows the variation of mean free path with pressure in a typical vacuum system.

5.2.0 SUBSTRATES:

5.2.1 CHOICE OF SUBSTRATES:

Two types of substrates were used for the deposition of thin Silicon Nitride films. One was Silicon (Si) because of its low cost, its involvement in the practical devices to be passivated and its mature technology. The other substrate used was Glass slide (25 mm sq, Corning).

Silicon was selected as the substrate to study

the optical transmission and electrical conduction mechanisms in thin Silicon Nitride films, whereas Glass was selected to study the relationship between the color and the thickness of the deposited Silicon Nitride films. Si was used as the substrate for the fabrication of MIS capacitors and Glass was used as the substrate for the fabrication of MIM structures. Actual steps involved in the fabrication are described in section 5.3.0.

5.2.2 ETCHING OF SUBSTRATES:

(a) SILICON:

Silicon substrates carry approximately 5-10 nm thick layers of native oxide which must be etched away before deposition. Best results were obtained by following the procedure listed below.

(i) Ultrasonic Deionized water bath for 30 minutes.

(ii) Dry with He spray and etch for 30 minutes in HF (48 %) under a venting hood.

(iii) Rinse in Methanol in two seperate baths, rinse in Trichloroethylene and finally rinse in two seperate baths of Isopropanol.

(iv) Ultrasonic Isopropanol bath for 15 minutes.

(v) Transport substrates to intervac immediately after blowing dry the samples with He.

(b) GLASS:

Glass substrates were cleaned in the ultrasonic bath of Isopropanol for 15 minutes and then were transported to intervac chamber immediately after blown dry with He.

The Silicon substrates used were P-type with <111> orientation having 70-90 ohm-cm resistivity. Their shape was triangular, cut from a 42 mm diameter Si wafer. Six substrates could be obtained from one such wafer.

Stainless steel masks were used on certain substrates so as to facilitate thickness measurement and deposition of electrode material. These masks are shown in Figure 5.2.

5.3.0 DEPOSITION PROCESS:

The process employed for the deposition of Si_3N_4 thin films can be explained in five basic steps:

I PREPRATION OF THE SYSTEM FOR FILM DEPOSITION:

It is a well established fact that quality of the film to be deposited depends upon the impurities picked up during actual sputtering (which also include trapped moisture in the chamber), cleanliness of the vacuum chamber, presputtering vacuum (base pressure or background pressure) etc. Quality of the films can be positively

improved by reducing the contamination and improving the presputtering vacuum. To reduce the contamination, vacuum chamber should be thoroughly cleaned, at the most, after seven deposition runs. Since vacuum chamber wall absorbs moisture from the atmosphere, it is desired that chamber should not be opened and/or left open for longer durations than necessary. Whenever the system is not used for the deposition it must be left under vacuum except for cleaning or trouble-shooting (unavoidable). Following is the step by step procedure followed for the film deposition, assuming that the system was cleaned prior to deposition.

INITIAL PUMPDOWN (Assuming that cryopump was running):

(i) With the roughing and high vac valves closed, the roughing line was pumped down to approximately 50 mtorr.
(ii) Roughing valve was opened and the main chamber was evacuated with the mechanical pump to approximately 50 mtorr.
(iii) Roughing valve was closed, high vac valve was opened and the system was left in this condition overnite.
(iv) Intervac roughing switch was then set "ON" and the intervac chamber was kept roughed.
(v) System was thoroughly checked for leaks, with He, using Residual Gas Analyser (RGA). Vacuum rise time was checked as described earlier in this chapter.

II SUBSTRATE PREPRATION:

After about 24 hours of evacuation, substrates were prepared for the deposition of Si_3N_4 as described in section 5.2.2.

III TRANSPORTATION OF SUBSTRATES TO THE MAIN VACUUM CHAMBER:

This was among the most critical steps in the deposition process, since the chemically etched substrates were exposed to atmosphere and probability of their getting contaminated while being transported from Isopropanol to Copper pallet in the intervac chamber is very high. Transporting of these substrates involved a complex sequence of panel controls listed below:

(i) After the substrates were laid on the platen (masks too), intervac chamber was pumped down to attain its ultimate vacuum (10 mtorr). Substrate arrangement was drawn in the laboratory note book for later referance, during this pumped down duration.

(ii) Anode was lowered and the stainless steel shield (this shield was used only in earlier runs) was pulled out of the way and the ionization gauge was set in 10^{-4} range. Desired target was positioned to be sputtered, using the index

wheel.

(iii) Intervac door was tripped to open and the plunger (carrying the substrates on the platen) was moved in.

(iv) Anode was raised to its upper limit when the plunger was all the way in.

(v) Plunger was retracted.

(vi) Anode height was adjusted as desired.

Speed at which the plunger was moved "IN" or "out" was very critical because if the speed were too high, the position of the substrates and the masks on the pallet could change and if it were too low, the main vacuum chamber and the substrates were exposed to intervac impurities for longer duration of time. Furthermore, it is very important to synchronize the motion of plunger and intervac door. It was a matter of experience to adjust and tune the pneumatic intervac mechanism using the air valves on the left side of the main chamber, behind the intervac control panel. Sputtering was never done without the platen on the anode since a film could be deposited on the anode insulator, causing a short circuit of anode to the system if the target sputtered was metallic.

After careful insertion of the substrates and the anode height adjustment, the stainless steel shield (presputtering shield) was used to cover the substrates. The chamber was then evacuated for atleast 2-3 hours before

proceeding to actual deposition. It was never attempted to commence sputtering if the pressure in the main chamber was higher than $2*10^{-6}$ torr (presputtering pressure) for Si_3N_4 deposition. After the vacuum in the main chamber was below $5*10^{-6}$ torr, ionization gauge was degassed for 40 seconds and He leak detection was performed using RGA (whenever possible) after 30-45 minutes (depending upon the vacuum).

At this stage, all the water valves were checked to ensure proper settings for the efficient cooling of the system fixtures during the deposition run. These settings were:

(i) The activated charcoal filter that filters the main cold water supply to the system, was flushed.

(ii) Main anode cold water valve was kept open to provide the substrate cooling.

(iii) Anode o-ring cold water valve was kept open to cool the anode insulator.

(iv) Cold water supply to targets, filament boxes and filament feed throughs was kept "ON".

(v) Pallet (intervac) water valve was kept "ON".

(vi) Load resistor cooling was "ON".

(vii) To assure that water was flowing through its paths without any obstacles, the drain lines for all the above mentioned components were checked constantly.

IV FILM DEPOSITION:

This was very critical and every possible precaution was taken. Following is the procedure to initiate the plasma and then sustaining it with the desired parameters.

(1) Range on the ionization gauge was switched to 10^{-4} torr and Ar gas was introduced into the main chamber through the micrometering valve to build up a partial pressure of 10^{-4} torr. Range on ionization gauge was then switched to 10^{-2} torr.

(2) Circuit breakers for RF power generator, filament current and DC power supply were turned on.

(3) Filament current was increased in the steps of 5 amps after every 2 minutes until 60 amps were reached. Triode power supply voltage (DC) was increased for anode potential to attract electrons emitted by the triode filament and was adjusted for about 100 volts. At this stage sputtering pressure was increased to $2*10^{-2}$ torr. For Ar as sputtering gas, a bright plasma appeared at this stage and the plasma current (DC current) was adjusted with the minor adjustments of filament current and DC power supply. Normally these two were adjusted for saturation of filament as explained in the manual, for the system, available in the laboratory. However, if the on-set of the plasma did

not occur at this stage then an attempt was made to ignite the plasma with RF power. In this case with yellow standby light of the Rf generator "ON", the red power switch was depressed and the RF drive was increased. Immediately plasma should appear. If it takes more then 3 minutes to initiate the plasma, it is advisable to repeate the procedure after switching the RF generator to standby mode, DC triode voltage and filament current to zero and closing the micrometering valve. Time consumed in initiating the plasma is extremely critical since if the high gas pressure is maintained for more then 3 minutes, cryopump might require regeneration, resulting in undesirable delay and the entire deposition process might need to be repeated.

Once the plasma is ignited, it was sustained at lower pressures. Quickly the pressure was reduced to the desired value and RF drive was adjusted to get the desired forward power. In any case, reflected power should not exceed 75 watts. Higher reflected power (>75 watts) could cause expensive as well extensive damage to the RF generator. Then, the matching networks for the target were tuned to obtain maximum forward and minimum reflected power. It was a matter of experience to achieve the best tuning for each run. After achieving the best tuning, all the parameters were precisely adjusted to the desired values with slight adjustments required in tuning. Special

attention was given to the forward power since it was directly related to the deposition rate. Further, excessive target heating is also undesirable which is caused by higher RF powers. In cases where the plasma was flickering, its stabalization was achieved by either retuning or varying the sputtering pressure or filament current. If the flickering still persists, it is usually an indication of dirty system. However, it was rarely observed for the sputtering pressures between 2-9 mtorr. Plasma was usually violet, bright and well confined.

Presputtering shield was removed only after the stable plasma was attained. This shield served several important functions such as preventing the deposition of sputtered material on to the substrates during the inital set up of plasma and for presputtering the target. With the steady plasma and shield removed, deposition was carried out for the desired length of time and the sputtering parameters were noted down and varified after every 5 minutes.

There were few parameters which needed regular attention and were kept constant during the run are described below.

(a) DC plasma current was 2.5-4 amps and filament current was 58-61 amps. As mentioned earlier, filament was adjusted for saturation, i.e., an increase in filament current

should not increase the DC plasma current.

(b) Sputtering pressure measured on the ionization gauge was kept constant, with in + 1 % accuracy of the desired value.

(c) RF forward and reflected powers were tuned for maximum efficiency and minimum mismatch between generator and load.

V SPUTTERING SHUT DOWN:

This step of film deposition was as important as any other step and its mishandling could adversely influence the film properties.

After the timer automatically switched the RF generator into standby mode, RF drive was set to zero, timer switch was reset to continuous sputtering, and the micrometer valve was closed tightly.

Filament current was lowered by 5 amps every 2 minutes whereas DC triode voltage was reduced in steps of 10 volts every 2 minutes simultaneously, until both of them reached zero. Circuit breakers for RF generator, filament current and DC power supply were turned off. The substrates were then brought back to the intervac chamber, with the help of pneumatic control, after allowing the substrates to be cooled for approximately 50 to 75 minutes.

5.4.0 FABRICATION OF MIS AND MIM CAPACITORS:

For the fabrication of MIS capacitors, certain substrates (with Si_3N_4 film on it) were selected for metallization. Niobium (Nb) was sputtered after masking the samples appropriately. Niobium was selected basically for the reason that the Nb target was available in the laboratory and from the device point of view, it provided ohmic contact on Silicon which was required.

Electrode areas used were $7.068*10^{-2}$ sq-cm and $6.36*10^{-3}$ sq-cm. In many cases Aluminium (Al) was evaporated instead of Nb. Various steps involved are shown schematically in Figure 5.3. Fabrication of MIM structure was exectly identical except for Nb deposition prior to Si_3N_4, on glass substrate.

5.5.0 DEPOSITION OF a-Ge FILMS:

Amorphous Germanium films were prepared by direct RF sputtering of Germanium target. Substrates used were again p-type Si and Corning Glass slides. Details regarding the properties of these substrates and their preparation for sputter deposition were identical to those of substrates used for Si_3N_4 films and are discussed in sections 5.2.1 and 5.2.2 of this chapter. Apart from these substrates, five nuclear detectors (supplied by P.G.T.)

were also passivated under different atmospheres. These depositions were carried out in either Ar/H or Ar-H mixture. Deposition procedure was exactly identical to one described earlier in section 5.3.0. Various deposition conditions used for passivation of nuclear detectors are tabulated in Table 6.3. Experimental conditions of some of the other runs are given in Table 6.2.

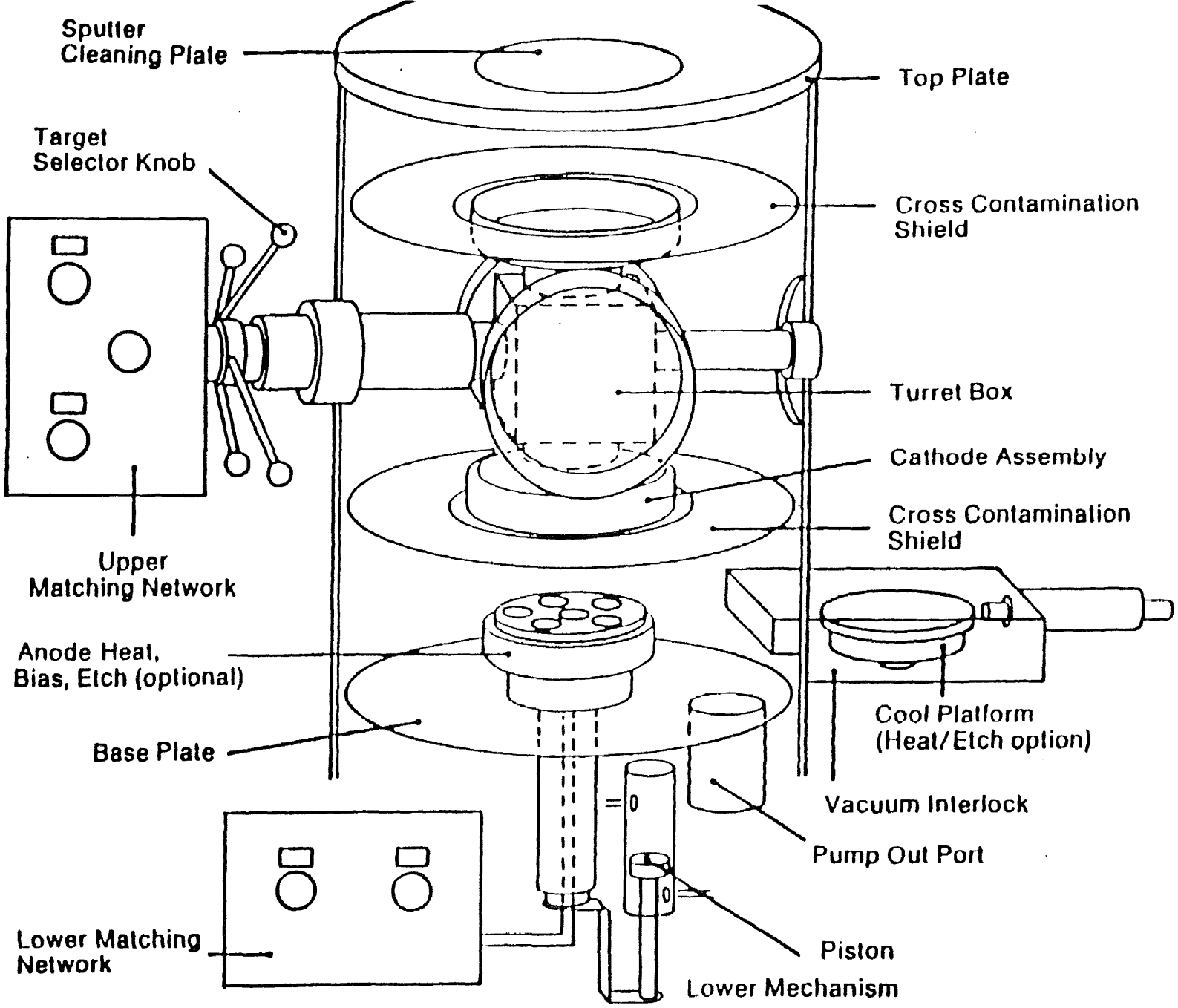

Fig. 5.1 MRC 8800 SPUTTERING SYSTEM.

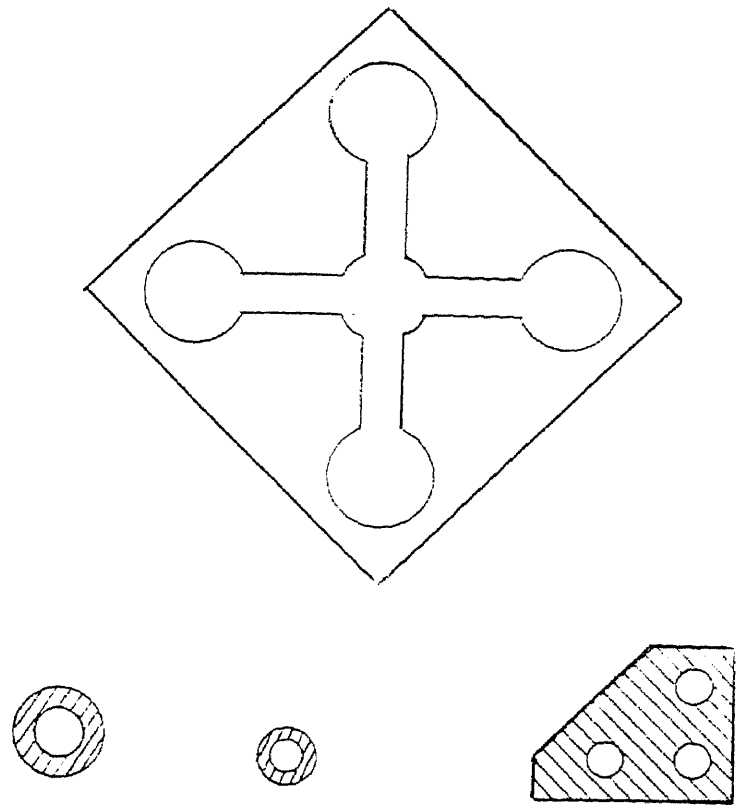

Fig. 5.2 MASKS

A) CLEAN SUBSTRATE PREPARED FOR DEPOSITION.

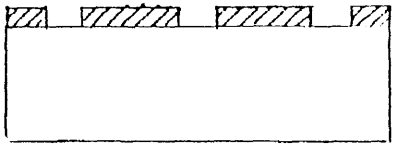

B) MASKED SiN DEPOSITION.

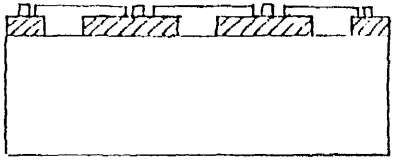

C) MASKED METTALLIZATION OVER SiN.

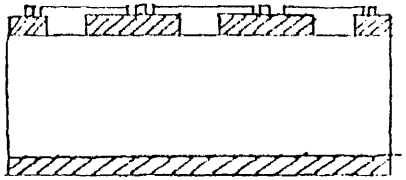

D) METTALLIZATION FOR OTHER ELECTRODE.

Fig. 5.3 MIS: STEPS IN FABRICATION.

Pressure (torr)	mean free path (cm)	collision/sec. (between molecules)	molecules/sec. (striking surface
10^{-2}	0.5	9×10^{4}	3.8×10^{18}
10^{-4}	51	900	3.8×10^{16}
10^{-5}	510	90	3.8×10^{15}
10^{-7}	5.1×10^{4}	0.9	3.8×10^{13}
10^{-9}	5.1×10^{6}	9×10^{-3}	3.8×10^{11}

Table 5.1 High Vacuum Conditions

VI EXPERIMENTAL DATA AND RESULTS

6.1.0 INTRODUCTION:

Deposition conditions affect the film properties significantly and these properties can be varied in a controlled manner by controlling the deposition parameters. For sputter deposition, these parameters are sputtering pressure, power density, target-substrate spacing, temperature etc. Apart from these experimental parameters, film properties are markedly affected by pre and post deposition conditions also.[41] These are pre-sputtering pressure, substrate cleaning, past history of the sputtering system (conditions of the system prior to deposition), film treatment immediately after the deposition etc. Thus it is very important to plan the experiment well in advance.

Experimental conditions and results obtained are presented in this chapter. An explanation for the results obtained is presented in next chapter.

6.2.0 EXPERIMENTAL DATA:

6.2.1 SILICON NITRIDE:

This Author had conducted over 90 experiments for this study, 70 on Nitride. Due to lack of time, it is not

possible to reprint experimental data for all those runs but a few of them are presented in this chapter. Each set of data represents an individual run. Deposition conditions for the remaining runs are available from the Drexler Microelectronics laboratories upon permission of supervisors of this research.

Deposition conditions for Si_3N_4 from ten runs are listed in Table 6.1.

6.2.2 a-GERMANIUM:

Deposition conditions for a-Ge on Si and Glass are listed in Table 6.2, whereas Table 6.3 contains the deposition conditions used for nuclear detectors.

6.3.0 RESULTS:

6.3.1 SILICON NITRIDE

Silicon Nitride films were evaluated by their dielectric constant, I-V curves and IR responses. All these properties were found to be remarkably dependent upon the sputtering conditions. Influences of these conditions on the properties of Si_3N_4 are discussed in context to the results obtained in the next chapter. Sample calculations are explained in this section.

6.3.2 DIELECTRIC CONSTANT:

(a) calculation from capacitance:

Dielectric constant was calculated from the basic relation

$$C = A\epsilon_o\epsilon_r/d \qquad \text{------(6.1)}$$

where C = Capacitance (Farad),

A = Area (sq-cm),

ϵ_o = Permittivity of vacuum = $8.854*10^{-14}$,

ϵ_r = Dielectric Constant of the film,

d = Film Thickness (nm).

C was mesured from L-C-R bridge as explained in the section 7.4.0 and d was calculated using the angstrometer as per section 4.2.0. All others are known except for ϵ_r. Sample calculation shown below is for R35S6. For this run, values are:

C = 8.4 nF,

A = 0.0706 cm^2,

d = 44 nm

ϵ_o = $8.854*10^{-14}$

Using these values in the equation 6.1, we get

$$\epsilon_r = \frac{440*10^{-8}*8.4*10^{-9}}{8.854*10^{-14}*0.0706}$$

$$\epsilon_r = 5.9$$

(b) Calculation from J - $\sqrt{E}$ curve:

Dielectric constant was also calculated from the conduction curves (J - $\sqrt{E}$) and it was found that the values obtained using this method were approximately same as those obtained by using capacitance which is explained above. Sample calculation is shown below.

Theoretical value of Poole-Frenkel coefficient is given by

$$B_{PF} = (q/\pi\epsilon_0\epsilon_r)^{1/2} \quad \text{--------(6.2)}$$

whereas the experimental value is given by

$$B_{PF} = (\text{slope})\ (kT/q) \quad \text{--------(6.3)}$$

Again consider the same sample R35S6 for which

slope = 0.0121

Thus equation 6.3 gives $B_{PF} = 3.15*10^{-4}$.

Now using this value in equation 6.2, it gives

$$\epsilon_r = 5.8$$

Dielectric constant values obtained from the two methods discussed above were consistent as shown in the Table 6.7.

(c) Calculation from Refractive Index:

Refractive index of these samples were determined from the IR response using a computer program.[45] Refractive index of these samples were found to be slightly higher than the bulk value and it ranged from 2.1 to 2.4. Dielectric constant was calculated from the optical

refractive index (n) using the relation

$$\epsilon_r = n^2 \qquad \text{----------(6.4)}$$

and dielectric constant thus calculated was found to be in the close agreement with that obtained from the two methods discussed earlier.

6.3.3 I-V CHARACTERISTICS:

These are conduction curves for Si_3N_4 films, obtained from plotting current density against square root of electric field. From these curves slope and conductivity were calculated as explained below.

SLOPE:

$$\text{Slope} = \frac{\Delta J}{\Delta E}$$

$$J = (\ln 10^{-3} - \ln 10^{-4})$$

$$= 9*10^{-4} \text{ amps/cm}^2$$

$$E = (1.3K - 1.11K)$$

$$= 190 \text{ V}$$

Thus slope = 0.0121

RESISTIVITY:

$$\text{Resistivity } (\rho) = \frac{E}{J}$$

$$J = 2.5*10^{-7} \text{ amps/cm}^2$$

$$E = 0.25\text{MV/cm}$$

Thus $\rho = 1.56*10^{12}$ ohm-cm

CONDUCTIVITY:

$$\text{Conductivity} = 1/\rho$$
$$= 6.4*10^{-13} \text{ mho/cm}$$

These results are listed in the Table 6.4. These I-V curves as well as the calculated results were compared with the published results and found that the films studied in this research were reasonably good.

6.3.4 INFLUENCE OF CARRIER GAS ON THE FILM PROPERTIES:

It was studied by IR spectrophotometery. No influence of various sputtering parameters were observed except for carrier gas. IR transmission responses are shown in Figures 7.9-7.15 and are discussed in section 7.6.0. Various frequencies of interest are shown in Table 6.5.

It had been concluded from the IR spectra that the strong, broad absorption band at about 840 cm^{-1} shifts considerably in accordance with the carrier gas and the film thickness. The films were composed principally of amorphous Si_3N_4 but trace amounts of impurities like Hydrogen and Oxygen were also present and it is suggested

that these impurities are responsible for the displacement of Si-N absorption band.

6.3.5 GERMANIUM:

A number of experiments were performed to deposit amorphous Ge films under varying conditions and the films obtaind were analysed by X-ray diffraction and IR spectroscopy. X-ray diffraction demonstrated the amorphous nature of the films. IR transmission showed that the hydrogenated films had transmission in the range 1800 to 2000 cm^{-1}. An attempt was made to develop Hall-effect measurements. Conductivity measurements were conducted in the same way as were for Si_3N_4 films. These results are not available at the time of publication but could be obtained from the referance.[45]

However, a-Ge as well as a-Ge:H was also deposited ongamma-ray detectors which were tested by P.G.T. staff before and after the passivation, and encouraging results were obtained. These results are reproduced in Table 6.6.

These detectors were subjected to a series of tests to determine the surface stability. These include leakage current, depletion voltage and mechanical abrasion tests. These tests proved that the surface stability was improved by sputter passivation.

RUN #	DEP TIME (min)	SPUTTER PRESS (torr)	SPUTTER GAS (%Ar-N)	ANODE HEIGHT (inch)	POWER (watts)	CATHODE VOLTAGE (kV)
(T)34	30	6.00E-03	50-00	3.70	260	1.50
(T)35	15	6.00E-03	50-00	3.70	250	1.35
(T)40	30	5.00E-03	60-40	3.80	250	1.28
(D)59	10	5.30E-03	100-00	2.10	125	1.30
(D)84	20	6.20E-03	00-100	3.20	190	1.30
(D)85	20	6.20E-03	00-100	3.00	200	1.30
(D)87	20	6.00E-03	25-75	3.00	190	1.40
(D)89	25	6.00E-03	25-75	3.00	160	1.15

TABLE 6.1 EXPERIMENTAL CONDITIONS FOR SILICON NITRIDE FILMS

RUN #	DEP TIME (min)	SPUTTER PRESSURE (torr)	ANODE HEIGHT (inch)	POWER (watts)	CATHODE VOLTAGE (kV)	THICKNESS (nm)	DEP RATE (nm/min)
46	15	8.00E-03	3.00	180	2.00	85.00	5.6
47	5	8.00E-03	3.00	150	2.00	68.70	13.74
48	3	8.00E-03	3.00	150	2.00	-	-
49	3	8.00E-03	3.10	125	1.70	-	-
50	3	8.00E-03	3.10	125	1.60	-	-
51	3	8.00E-03	1.00	110	1.55	20.00	6.66
* 61	3	9.00E-03	2.30	125	2.00	-	-

* : Mixture of 93 % Ar + 7 % H was used in run # 61

Table 6.2 Experimental conditions for a-Ge films

RUN #	DEP TIME (min)	SPUTTER PRESSURE (torr)	ANODE HEIGHT (inch)	POWER (watts)	CATHODE VOLTAGE (kV)	THICKNESS (nm)	DEP RATE (nm/min)
52	4	2.20E-02	4.00	125	1.60	85.00	21.25
53	3	9.00E-03	4.00	125	1.75	68.70	22.9
* 62	2	1.10E-02	4.00	100	1.60	-	-
* 63	2	9.20E-03	4.00	125	1.80	-	-
* 64	2	9.40E-03	2.90	115	1.50	-	-

* : Mixture of 93 % Ar + 7 % H was used

Table 6.3 Experimental conditions for pssivation of Ge Nuclear Radiation Dectectors

SAMPLE NO.	SLOPE	RESISTIVITY (ohm-cm)	CONDUCTIVITY (mho/cm)
R34S3	2.42E-02	2.60E+11	3.8500E-12
R35S5	8.20E-03	2.50E+10	4.0000E-11
R35S6	1.21E-02	8.65E+10	1.1500E-11
R40S1C2	2.09E-02	6.76E+09	1.5000E-10
R85S4C1	1.96E-02	7.70E+09	1.3000E-10
R87S5	1.77E-02	1.60E+10	6.2500E-11
R89S2C2	7.60E-03	2.16E+10	4.6300E-11
X	1.70E-02	6.15E+11	1.5000E-12
Z	1.09E-02	5.63E+10	1.7700E-11
Y	1.15E-02	1.00E+11	1.0000E-11

TABLE 6.4 ELECTRICAL PROPERTIES OF SPUTTERED SILICON NITRIDE FILMS

Table 6.5 USEFUL GROUP FREQUENCIES

SiH	2100 to 2260 cm^{-1} 800 to 960 cm^{-1}	Strong Medium	The higher stretching frequencies are found when electronegative substituents such as Cl are also attached to the Si.
SiCl	460 to 650 cm^{-1}	Strong	When two or three Cl atoms are present, two absorptions occur. Hydrolyzable group.
SiOH	3960 cm^{-1} (free) 3200-3400 cm^{-1} (bonded) 830- 950 cm^{-1}	Weak Medium Medium	
SiOSi	1000 to 1130 cm^{-1}	Strong	Bonding constraints lower the absorption frequency; electronegative substituents on the Si raise it. Long chain siloxanes show two broad absorptions near 1020 and 1090 cm^{-1}.
$SiNH_2$	3480 and 3400 cm^{-1} 1540 cm^{-1}	Medium Medium	Hydrolyzable group; reacts with CS_2
SiNHSi	3390 to 3420 cm^{-1} 1170 cm^{-1}; 910-950 cm^{-1}	Medium Strong	Hydrolyzable group
$SiCH_3$	1250 to 1270 cm^{-1} 750 to 870 cm^{-1}	Strong Strong	Very characteristic
$SiCH_2CH_3$	1220 to 1240 cm^{-1} 1000 to 1020 cm^{-1} 945 to 970 cm^{-1}	Medium Medium Medium	
$SiCH_2CH_2CH_3$	1200 to 1220 cm^{-1}	Weak	
$SiCH_2Si$	1040 to 1080 cm^{-1}	Strong	
$SiCH{=}CH_2$	1590 to 1610 cm^{-1} 1400 cm^{-1} 990 to 1020 cm^{-1} 940 to 980 cm^{-1}	Medium Medium Medium Medium	
$SiCH_2CH{=}CH_2$	1640 cm^{-1}	Medium	
SiC_6H_5	1590 cm^{-1} 1430 cm^{-1} 1120 cm^{-1}	Medium Medium Strong	
$SiOCH_3$	2840 cm^{-1} 1190 cm^{-1} 800 to 850 cm^{-1}	Strong Strong Medium	Hydrolyzable group
$SiOCH_2CH_3$	1160 to 1175 cm^{-1} 1100 and 1075 cm^{-1} 940 to 970 cm^{-1}	Medium Strong Medium	Hydrolyzable group
$SiOCOCH_3$	1700 to 1770 cm^{-1} 1190 to 1250 cm^{-1} 1000 to 1050 cm^{-1}	Strong Strong Strong	

Table 6.6

EPGT **Sputtering Results**

(Pure Argon, 20mm Hg pressure, 10 minutes approx 100 angstrom thick)

1. Detector S/N 1186, p-type , 46%

Date	Treatment	Results
9/15/86	Implanted and surface passivated(20 sec in H_2O_2)	In test cryostat, forward resistance 8kohms @ 4000V, -0.2, 15 mV @ 5000V, -0.3, 20 mV
11/10/86	Sputtered	Forward resistance 7kohms @ 4000V, +0.10, 70 mV @ 5000V, cryostat breakdown
11/15/86	Transferred to cooled-FET crystal	@ 4000V, -0.4, 14 mV @ 5000V, -1.50, 20 mV(+ pos spikes)
11/21/86	Exposed to water vapor and rosin-core smoke	@ 4000V, -0.4, 13 mV(+ pos spikes) @ 5000V, -1.6, 20 mV(+ pos spikes)
12/08/86	Wiped with methanol-soaked tissue,left stains	@ 4000V, -10V, 25 mV @ 4500V, -15V, 25 mV
12/10/86	Methanol wash	@ 4000V, -5.5V, 17 mV @ 5000V,-8.0V, 17 mV(+pos spikes)

2. Detector S/N N-244, planar 2000 x 16, new style

4/14/86	Implanted and surface passivation(15 sec in H_2O_2)	In test cryostat, forward resistance 10kohms @ 3000V, -0.30, 14 mV @ 4000V, -0.25, 18 mV
11/10/86	Sputtered	In test cryostat, forward resistance 6kohms @ 3000V, -1.03, 18 mV @ 3500V, -0.95, 18 mV
11/15/86	Transferred to cooled FET cryostat	@ 3000V, +1.40, 9 mV @ 4000V, +3.00, 10 mV
11/21/86	Exposed to water vapour and rosin fumes	@ 3000V, +1.50, 9 mV @ 4000V, +3.00, 9 mV
12/08/86	Methanol wash while in holder, stains	@ 2000V, +0.75, 8 mV @ 3000V, +4./50, high
12/10/86	Methanol wash	@ 2000V, +1.40, 10 mV @ 3000V, breaking

SAMPLE #	DIELECTRIC CONSTANT	
	FROM CAPACITANCE	FROM SLOPE
R35S6	5.9	5.8
R41S2C2	6.1	6.4
R41S1	5.8	5.2
R41S4	7.83	7.75

TABLE 6.7 DIELECTRIC CONSTANT OF THE OF SILICON NITRIDE FILMS USING VARIOUS METHODS

VII DISCUSSION OF RESULTS

7.1.0 INTRODUCTION:

Silicon Nitride films were deposited in Ar/N_2 or $Ar-N_2$ mixture plasma using direct RF sputtering of Si_3N_4 target (99.99%). Deposition rate and electrical properties of these films were studied as a function of sputtering parameters. IR spectrophotometery was used to analyse the influence of carrier gas on the composition of the films. Results of conductivity measurements are discussed in detail. Due to scarcity of results on direct sputtered Si_3N_4 in literature, author has compared his results with those of reactively sputtered and CVD films by various workers. Remarks made in this thesis are very priliminary and author believes that more research is needed to establish the growth behavior of direct sputtered Si_3N_4 films.

7.2.0 EFFECT OF SPUTTERING PARAMETERS:

Various parameters studied were Power Density, Sputtering Pressure, Carrier Gas and Deposition Time. Effect of film thickness on dielectric constant is also analysed. Detailed discussion on results is presented in this chapter.

7.2.1 POWER DENSITY AND DEPOSITION TIME:

Deposition rate was found to increase with power density (Figure 7.1). Although, in some cases, high deposition rates were observed for lower power densities. It is suggested that deposition time plays an important role in determining the deposition rate. As seen from Figure 7.2, deposition rate is found to be exponentially decreasing with the increasing deposition time irrespective of power density. Author argues that although higher deposition rates are expected at higher power densities but at the same time temperature of the cathode (target) also increases at higher power densities applied for longer duration of time and deposition rate decreases with the increasing cathode temperature. Thus indirectly cathode temperature controls the deposition rate.

7.2.2 CARRIER GAS:

Deposition rate was found to be very sensitive to the deposition ambient. Higher deposition rates were observed when Ar was used as carrier gas but it suffered greatly when N_2 was used. This is shown in Figure 7.3. Influence of carrier gas was also observed on the conductivity of the films. Films exhibited higher conductivity when deposited in Ar plasma as compared to

those deposited in N_2 plasma. It is attributed to preferential sputtering of the compound target and the films were found to be Si rich when deposited in Ar plasma. Influence of carrier gas on conductivity is discussed in detail in section 7.5.0. Effect of the carrier gas observed on the IR response is discussed in section 7.6.0.

7.2.3 SPUTTERING PRESSURE:

Deposition rate was relatively constant in the pressure range 4.5-6.5 microns and dropped off rapidly at the lower pressure end while dropped off slowly at the increasing pressure end. It is illustrated in Figure 7.4. It could be supported by the arguement that as this pressure increases, mean free path of the atoms travelling towards the substrates reduces due to the increase in the interatomic collisions. For very low pressures, there aren't enough atoms available to knock out the sputtered species in large numbers, thus resulting in lower deposition rates.

7.2.4 INHOMOGINIETY:

An important observation made during this research was that in some cases the films from the same deposition run exhibited strikingly different properties; an indication of inhomogeneous deposition. At times, various

samples from the same run had quite different film thicknesses, IR properties as well as different values of dielectric constant. However, the cause is not understood completely and needs more attention.

7.3.0 CORRELATION BETWEEN FILM THICKNESS AND DIELECTRIC CONSTANT:

Extensive evaluation of dielectric constant of Si_3N_4 films deposited under various conditions indicated that amorphous Si_3N_4films do not possess a unique value. It varied widely with the sputtering conditions and may range from 5 to 8. Effect of thickness on dielectric constant is shown in Figure 7.5. It was observed that dielectric constant increases with increase in film thickness as in agreement with Maes et al.[34] It may be an indication of increase in voids in the films.

7.4.0 CAPACITANCE MEASUREMENT:

Capacitance of MIS capacitors were measured using L-C-R bridge at 1KHz and 120 Hz. Samples were biased for accumulation mode so that the capacitance measured does not include the capacity offered by the substrate. Basic equivalent circuit for the MIS capacitor is shown in Figure 7.6.

Dielectric constant of the films was calculated as

explained in section 6.3.2. This calculated dielectric constant was found to be in the range from 5.0 to 8.0, but after about 15 hours of sputtering, the results were quite different which are discussed in the section 7.6.1.

7.5.0 I-V RESULTS:

To study the conduction mechanism in thin Silicon Nitride films, current-voltage relationship was established for metal-insulator-silicon (MIS) capacitors and was plotted in terms of current density versus square root of electric field (Figures 7.7 a & b). It was found that these films exhibited slightly higher conductivity than reported elsewhere in the literature.[21] On comparing the results on conduction characteristics of SiN films with those available in literature,[21,22,23] it was observed that the shape of the curve is similar but appeared to be shifted to the left. For comparison and better understanding, it is shown in Figures 7.7 a & b.

D.C. Resistivity and conductivity of these films were calculated from the current density versus square root of electric field plot as discussed in section 6.3.3.

Although the films were not of high quality, based upon the low fields and high current densities developed, it was interesting to note that the slope of the current density versus square root of electric field curve

was well in the range in which the slope of this curve was obtained by various researchers.[21,24] Comparison of these parameters (slope, conductivity and resistivity) obtained by author with those obtained by Sze[21] and Brown et al.[24] (Table 6.4) show that there is no significant descrepency in the electrical characteristics of the films studied in this research.

It would be necessary to confirm the self consistent effective dielectric constant in order to ensure the Poole-Frenkel type conduction in the Si_3N_4 films.[47] Table 7.1 shows the capacitance and the corrosponding dielectric constant values for the Si_3N_4 films as obtained experimentally. Taking the experimentally observed value of dielectric constant as 5.9, the calculated value of slope of the conduction curve (i.e., B/kT) is 0.0121. The experimenal value for the same is 0.0121 as observed from the J - $\sqrt{\mathcal{E}}$ curve. These calculations are explained in the chapter VI. This ensures self consistency in the relative dielectric constant value and thus conduction is believed to be of Poole-Frenkel type in the thin Si_3N_4 films. Similar observations had been reported by Sze,[21] Swaroop,[47] Deal et al[46] and a few others for Silicon Nitride films.

It was observed that the magnitude of the slope of the current density versus square root of electric field

curve was independent of the electrode material of the contact area. In this research, Niobium and Aluminium were used as the electrode material. The contact areas used were $7.068*10^{-2}$ sq-cm and $6.36*10^{-3}$ sq-cm. It was concluded that current density versus square root of the electric field characteristics (at room temperature) were independent of the electrode material, film thickness, and the device area, as reported by the other researchers.[21,24] But on the contrary while others have observed the independence of these characteristics on the polarity of electrode,[21,24] it was not so in this work. In this work it was found that in depletion mode (+MIS), the breakdown did not occur even at the fields of $5*10^{8}$ volts/cm, whereas in the accumulation mode (-MIS), the breakdown occurred at the fields of approx. 1 MV/cm. This early breakdown may be attributed to the large number of traps in the conduction band. Further it is believed by the author that the silicon nitride interface was not cleaned to satisfy the scientific standards. However, all precautions were taken to achieve optimum cleaning and it is an intuitive remark. Another remark is that incorporation of moisture in the films during the deposition. There was no facility available to measure or control the moisture trapped in the walls of the vacuum chamber. This is based on the results of the run performed after surface of the chamber was baked

by a heat gun for several hours thus outgassed prior to the deposition.

An explanation, for the controversial behavior mentioned earlier, regarding the dependence of current density versus square root of electric field characteristics on polarity is as follows. Silicon substrates used in this research were of P-type having resistivity of 70 ohm-cm, which is close to intrinsic semiconductor, whereas the substrates used by other researchers[21,22,23,24] were degenerate Silicon having resistivity in the range of 0.00005-0.01 ohm-cm. Thus in the case of depletion mode measurements, the discrepancy observed in the result could be attributed to this reason. In the case of degenerate semiconductor, Silicon substrate in fact acts like a metal whereas in case of high resistivity Silicon substrates, it is obvious to have high fields in depletion mode.

As far as the conduction mechanism in the Silicon Nitride films is concerned, due to independence of current density versus square root of electric field characteristics on the factors discussed above, it is suggested that the current is bulk controlled and conduction is electronic in nature. The conduction is in a form of field aided thermal ionization of trapping levels in the film, known as Poole- Frankle effect.

Electric fields developed in the films were much lower than those observed by others.[21,24] Author argues that it may be due to the higher Si/N ratio in his films as compared to that in the films studied by Brown et al,[24] who had reported that the curve shifts to the right (higher fields) as the Si/N ratio decreases. It is shown in the Figure 7.8. Films studied by him were prepared by Silane-Amonia reaction. Author has compared his results with those of Brown et al. even though films studied in this research were deposited by direct sputtering and this author wishes to inform the reader that this is an analogical conclusion and Si/N ratio measurement was not attempted.

7.6.0 IR TRANSMISSION SPECTROSCOPY:

Deposition was initially carried out in Ar plasma with varying sputtering pressures in the range of 1 to 9 microns. Invariably all the films exhibited broad classical Silicon Nitride absorption peak at approximately 840 cm^{-1} (Figure 7.9). IR response was indistinguishable in this pressure range. Later on the peak shifted and sometimes even the shape of IR response altered (Figure 7.10). After careful study of IR curves, it was determined that the films had incorporated moisture, Hydrogen and Oxygen during the deposition.

The strong absorption band of $Si_3N_4$was found to be

located at 840 cm^{-1}. Further, various functional groups associated with the Si-N absorption band were identified as Si-H, NH, SiO_x and Si-O-N_x. The NH stretching vibrations appeared at 3300 cm^{-1} whereas the absorption at 2300 cm^{-1} indicate the presence of weak Si-H stretching bond. These are shown in the Figures 7.10-7.12. It had been observed in a number of samples that broadening of the Si_3N_4 band near its baseline at 1170 cm^{-1} occurs with the presence of a weaker NH band at 3300 cm^{-1} (Figure 7.12). It is known that NH also has a symmetrical bending vibration near 1170 cm^{-1} so this broadening at 1170 cm^{-1} can be attributed to the NH, since it gets stronger as the NH absorption (3300 cm^{-1}) becomes more intense. It had been also observed that the main Si_3N_4 absorption band shifts to lower wavenumbers (from 840 cm^{-1}) with a stonger Si-H band (2300 cm^{-1}).

Actually the band does not shift but the profile of the band envelop changes due to the close proximity of another strong band.[42] The characteristic frequencies of bonds like Si-O, Si-H, Si-N, SiNH etc are in a very close range of 800 to 1100 cm^{-1} which increases the complexity in the analyses of the IR spectra of Si_3N_4 films.

These results provide evidence that the amorphous Si-N absorption band appears to shift because of the presence of unwanted Oxygen and Hydrogen concentrations. It has been suggested that presence of Hydrogen deteriorates

the physical and chemical properties of Silicon Nitride films. Further, Oxygen is supposed to contribute towards higher conductivity in Si_3N_4 thin films.

7.6.1 INFLUENCE OF CARRIER GAS ON THE IR RESPONSE:

Most significant observation of this research is the conclusion that stoichiometric silicon nitride films using direct sputtering of hot pressed silicon nitride target can not be obtained in argon plasma alone. It was observed that after 20 hours of sputtering this target in argon, slowly the infra-red absorption characteristics started altering and gradually the classical absorption diminished (Figure 7.13). At this stage, dielectric constant measured as described earlier also had reduced to approximately 3-4 indicating that the films were of silicon oxide and not silicon nitride. It was also noticed that the color of the target was dark gray at this stage while it was white initially. This observation was also confirmed from the literature available.[25] It is believed that the preferential sputtering of the Silicon Nitride target has occurred in only Argon plasma and in the later stages films were found to be Silicon rich. Author believes that the compositional changes have occurred in the target which could be now represented by an empirical formula of Si(x)N(y)H(p)O(q). It is assumed that due to porous nature

of this material, the target might have absorbed moisture as time passed by. Similar remarks had been made earlier by researchers like Vossen, to cite a reference.[26]

At this stage of research use of the Argon was discontinued and the vacuum chamber was purged with the Nitrogen gas (99.998 %) for two days and then the same target was sputtered in only Nitrogen for about 12 hours. An improvement was observed in the optical absorption and the dip was obtained. Subsequently the IR response became satisfactory (Figures 7.14&7.15). Later on a mixture of 25 % Argon (99.9995 %) and 75 % Nitrogen (99.998 %) was used for the deposition and the I-V results were found to be satisfactory. It is believed that Nitrogen was absorbed by the porous target and to a certain extent the films had improved. In fact it was reactive sputtering of Silicon Nitride target. Later, it was also observed that the color of the target was turning back to white.

However, with the availability of sensitive instrumentation such as Ellipsometry, Densitometer, C-V Plotter, FTIR etc., it will be possible to remark on physical and chemical properties of these films, in the future.

FIGURE 7.1 DEP RATE vs POWER DENSITY
6 mtorr

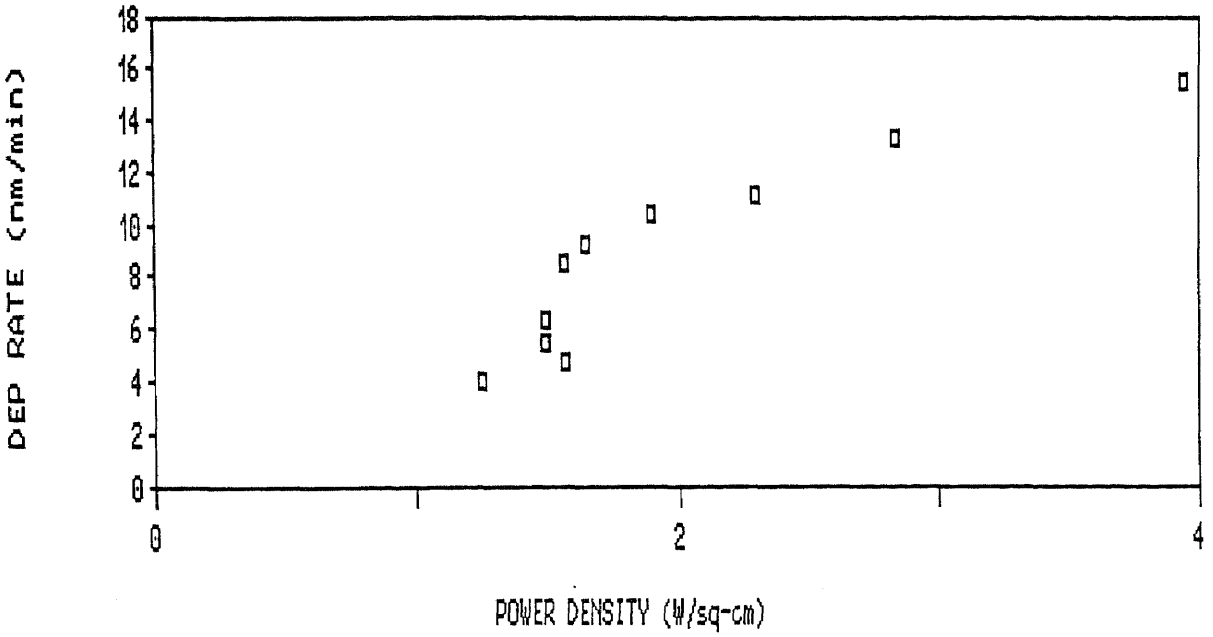

FIGURE 7.2 DEP RATE vs DEP TIME
200 WATTS, 6 micron

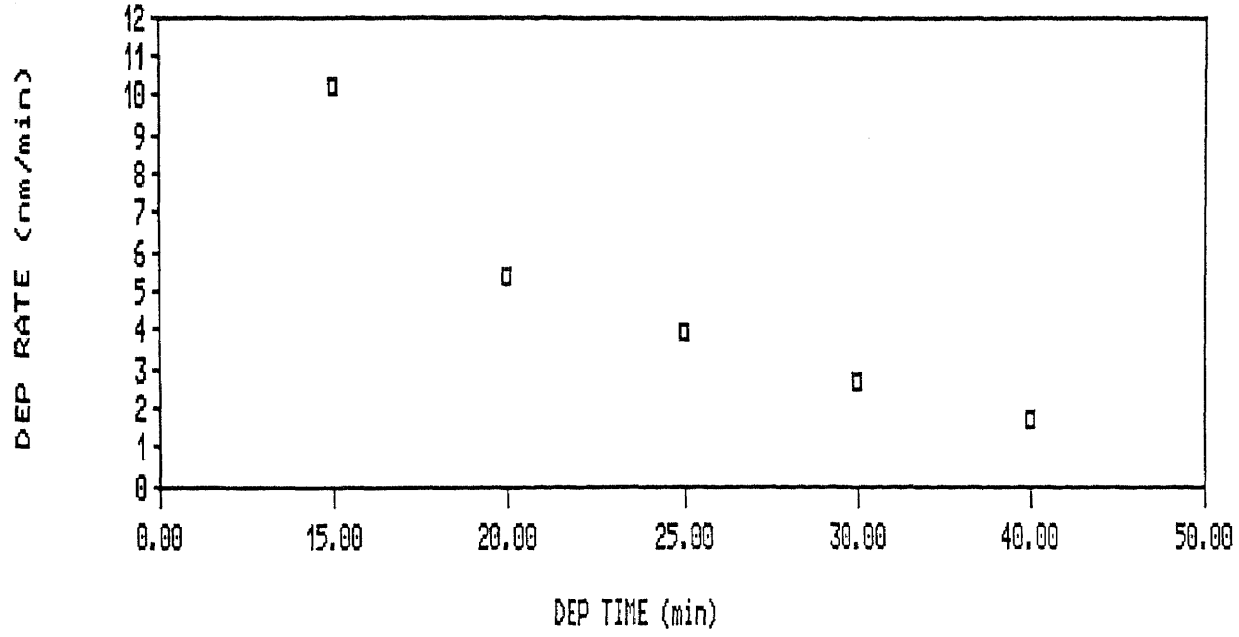

FIGURE 7.3 DEPOSITION RATE vs % N
200 WATTS

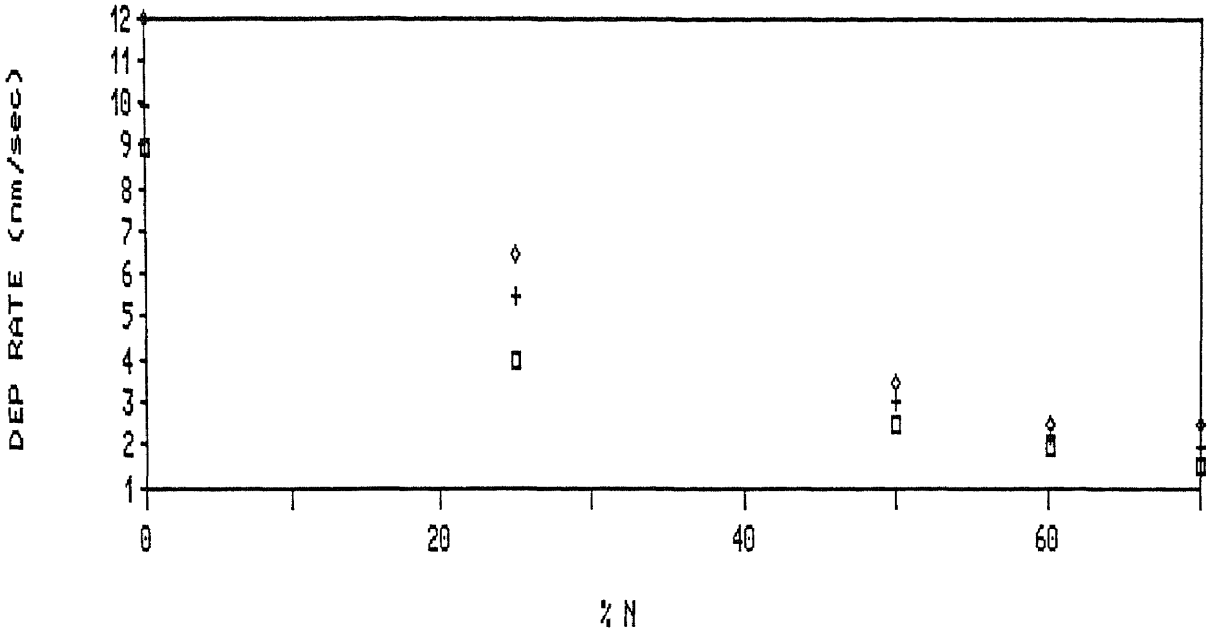

FIGURE 7.4 DEP RATE vs PRESSURE
(DIODE) 200 WATTS

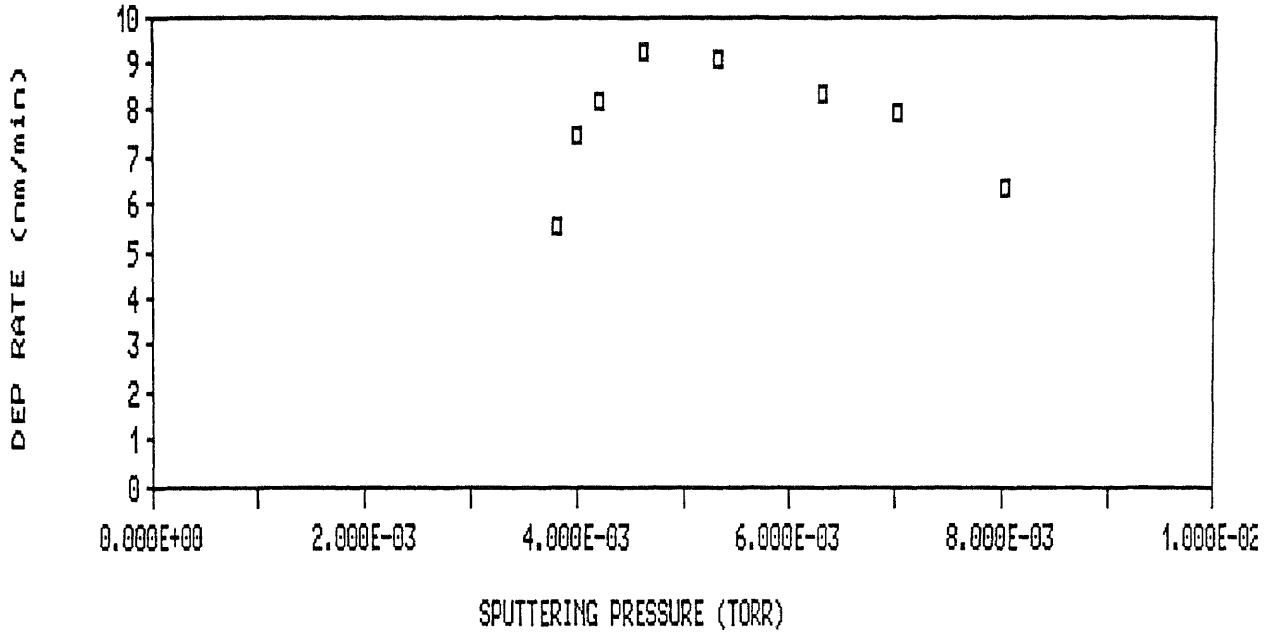

FIGURE 7.5 DIELECTRIC CONSTANT vs
FILM THICKNESS

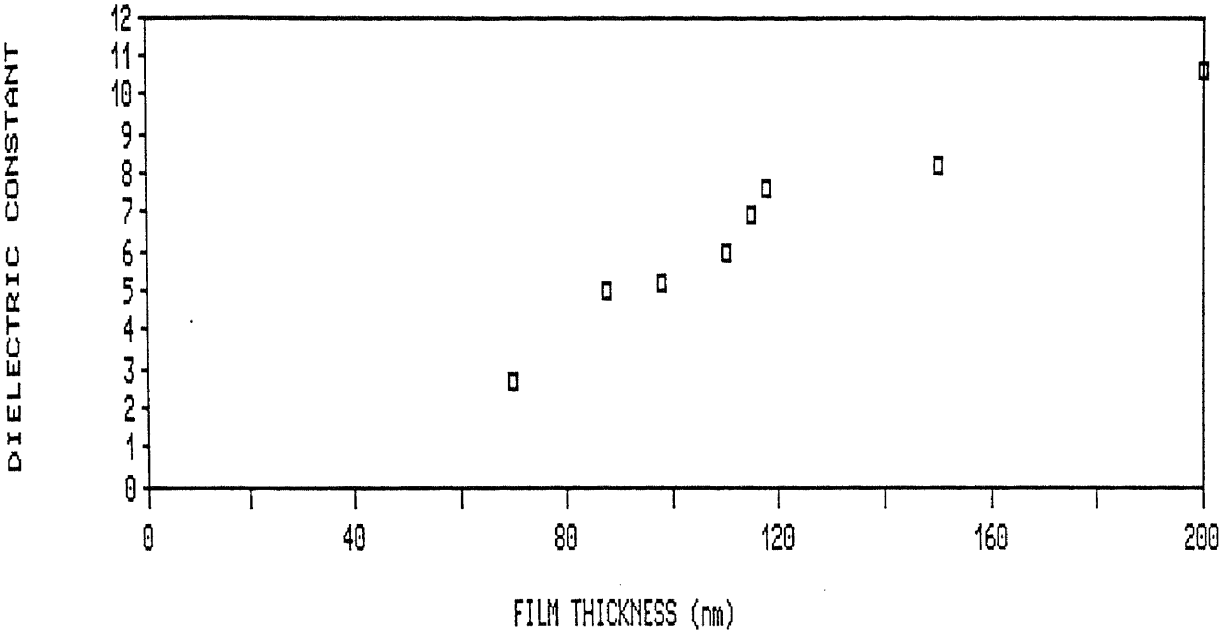

MIS CAPACITOR

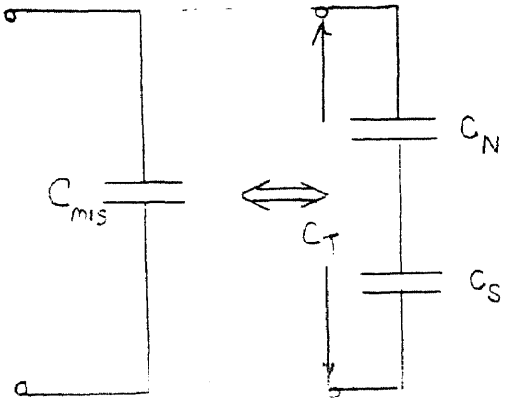

EQUIVALENT CIRCUIT.

$$C_T = \frac{C_N C_S}{C_N + C_S}$$

IN ACCUMULATION $C_S >> C_N$

$$\Rightarrow C_T = C_N$$

Fig. 7.6 EQUIVALENT CIRCUIT FOR MIS CAPACITOR

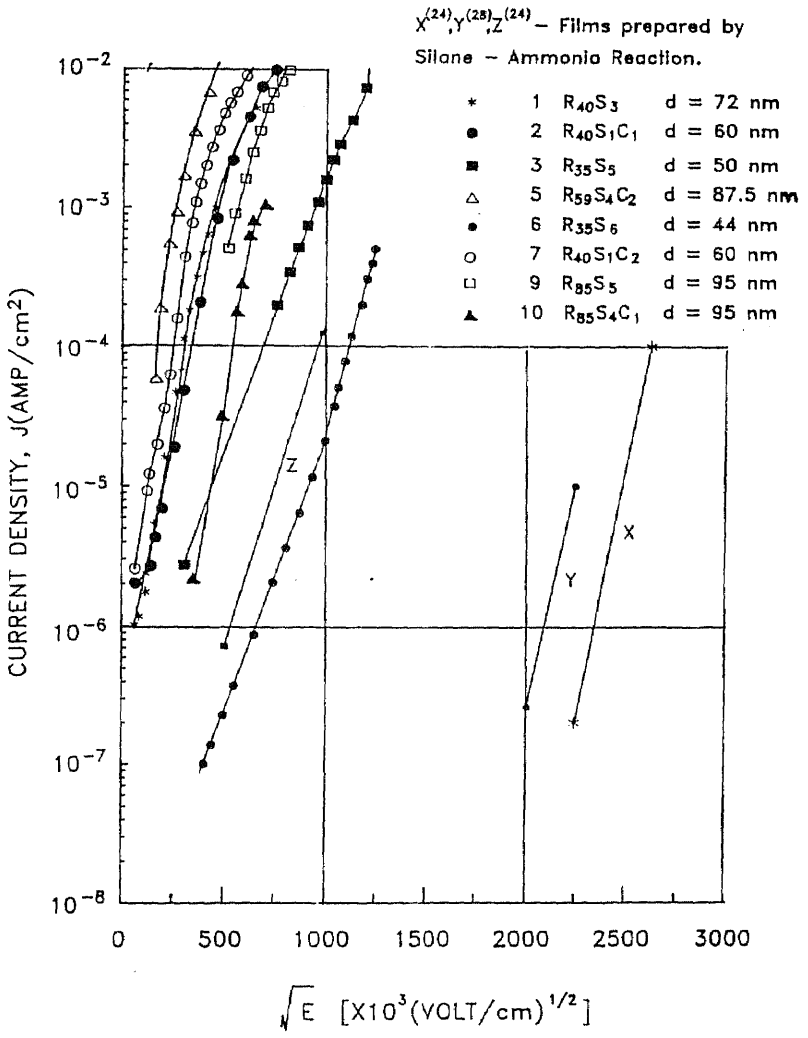

Fig. 7.7a Current density vs. square root of electric field in Silicon Nitride films.

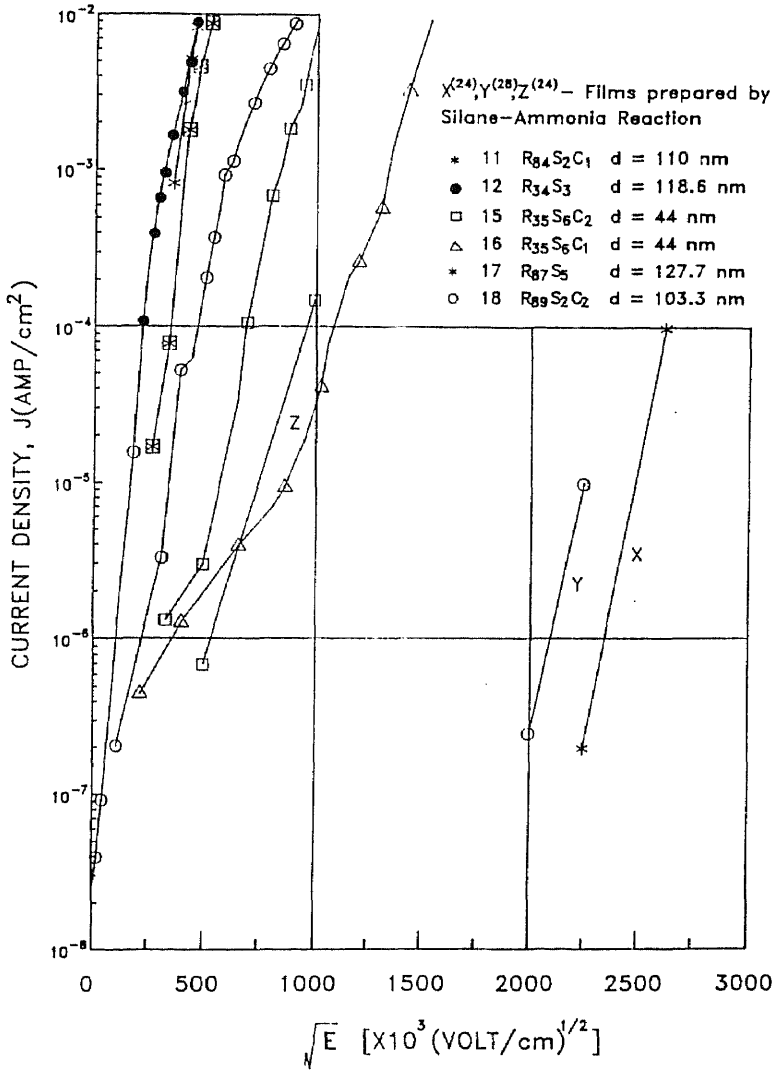

Fig. 7.7b The current density .vs. square root of electric field in silicon nitrate films.

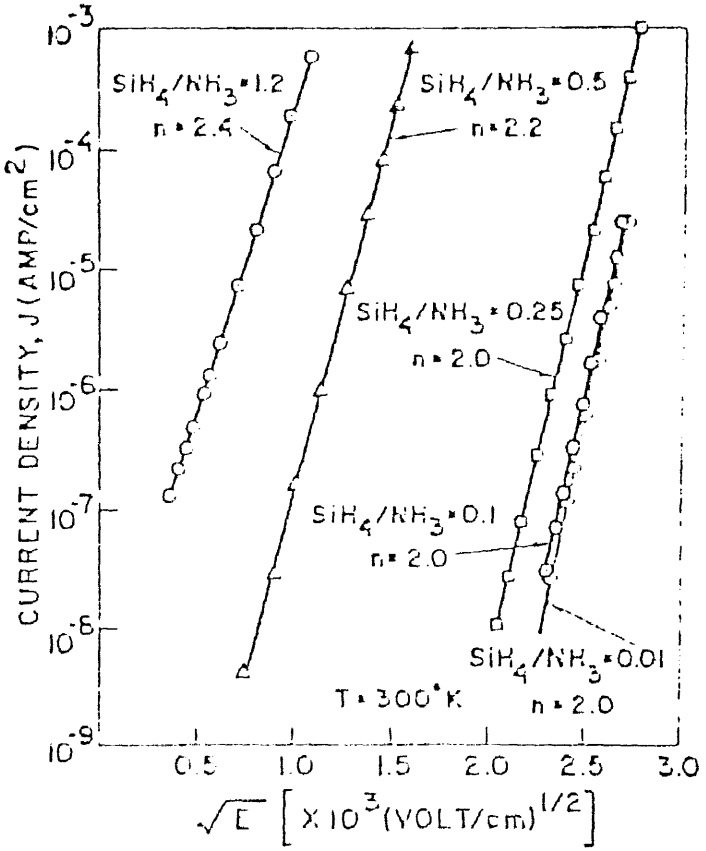

Fig 7.8 Log current density plotted vs. the square root of the electric field, showing the dependence of conductance on silane-ammonia ratio.

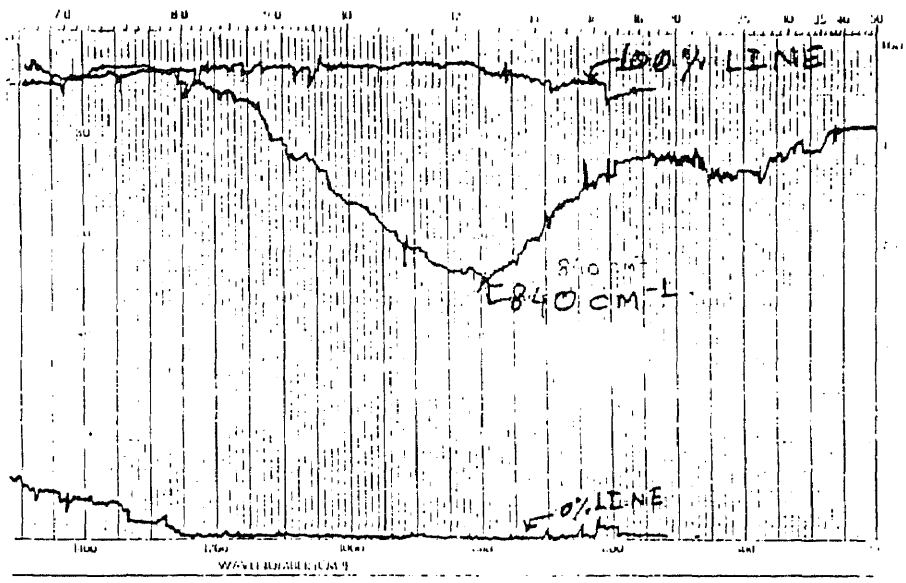

Fig. 7.9

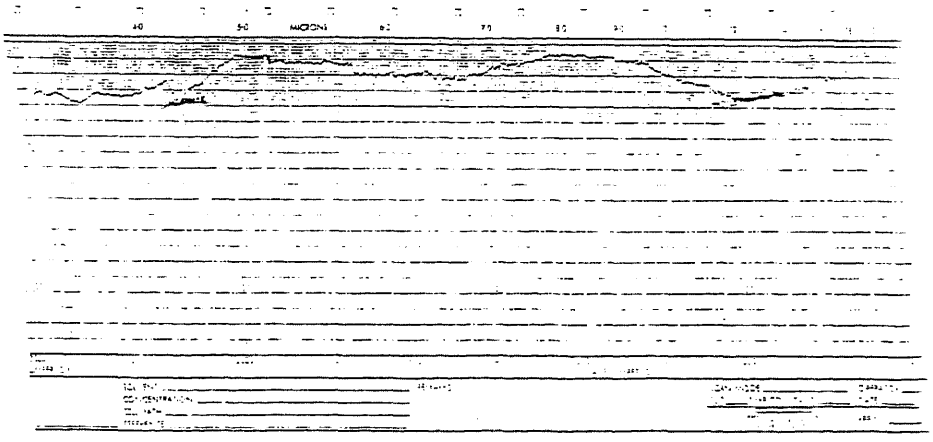

Fig. 7.10

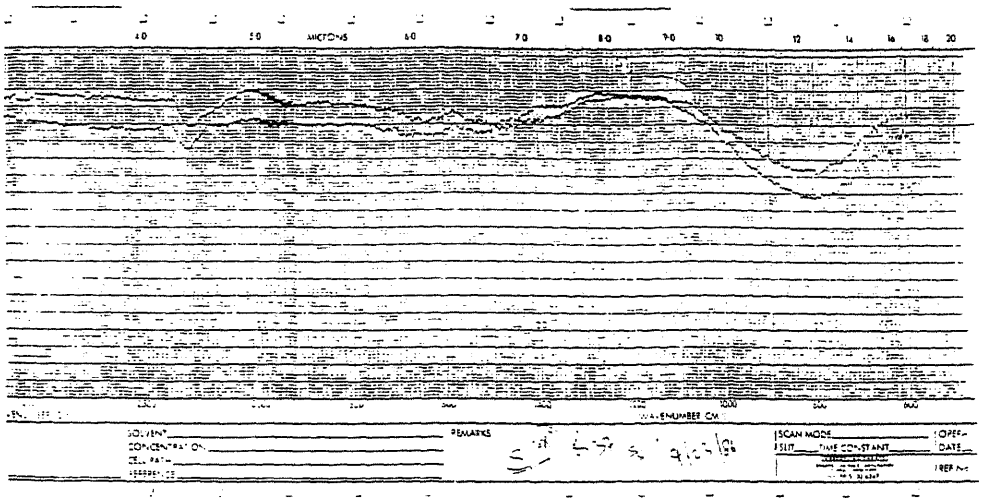

Fig. 7.11

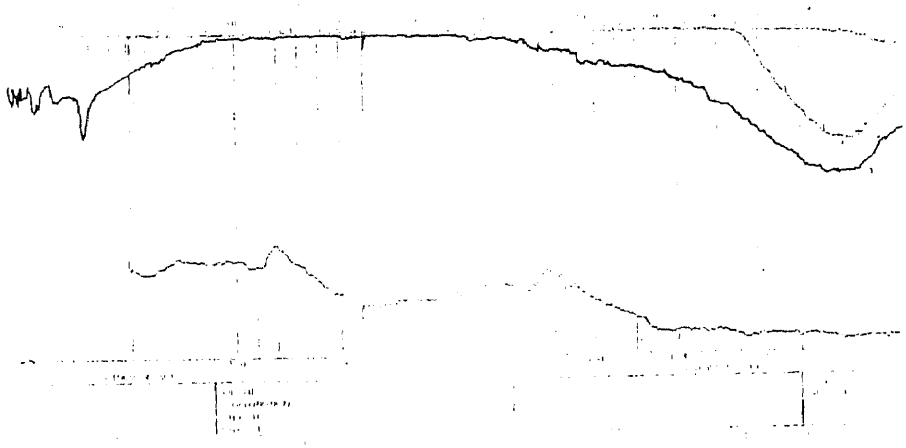

Fig. 7.12

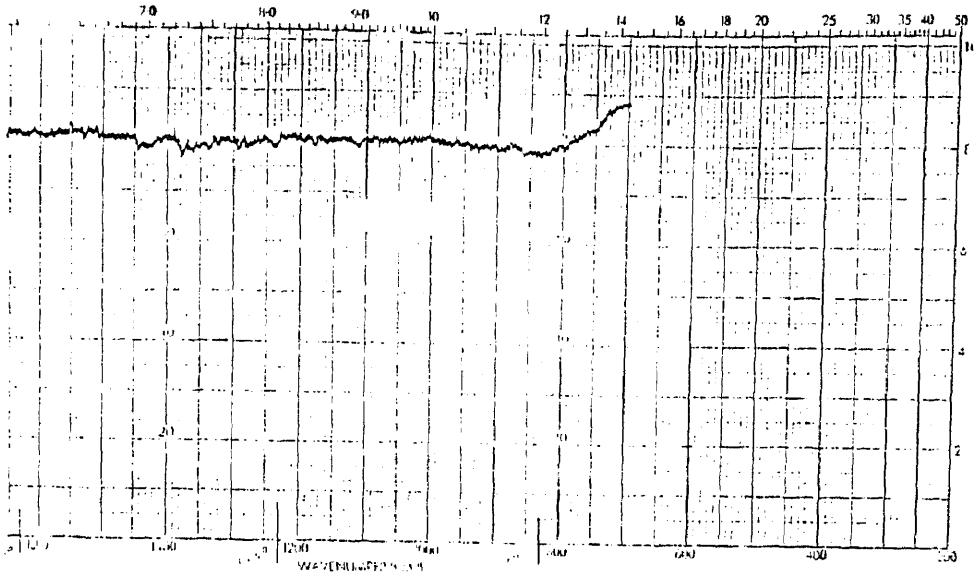

Fig. 7.13

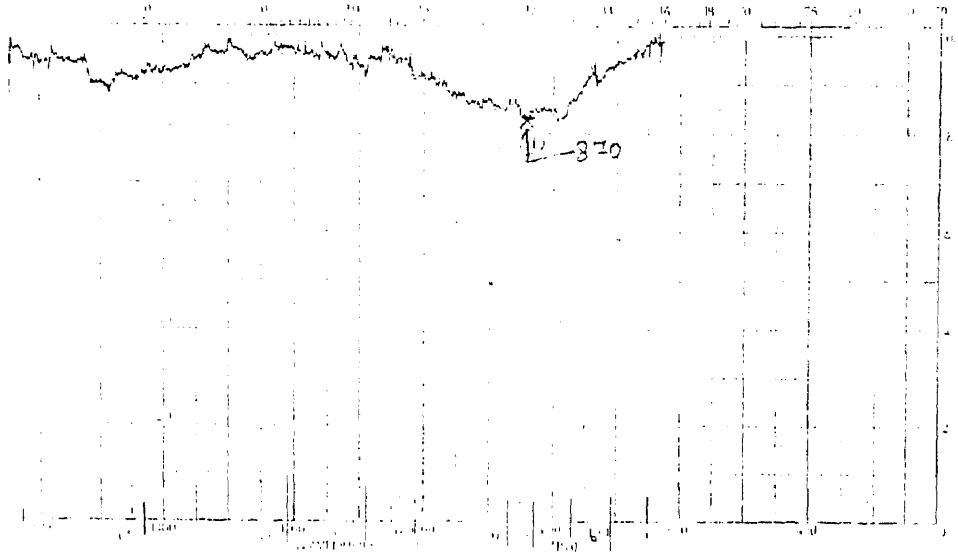

Fig. 7.14

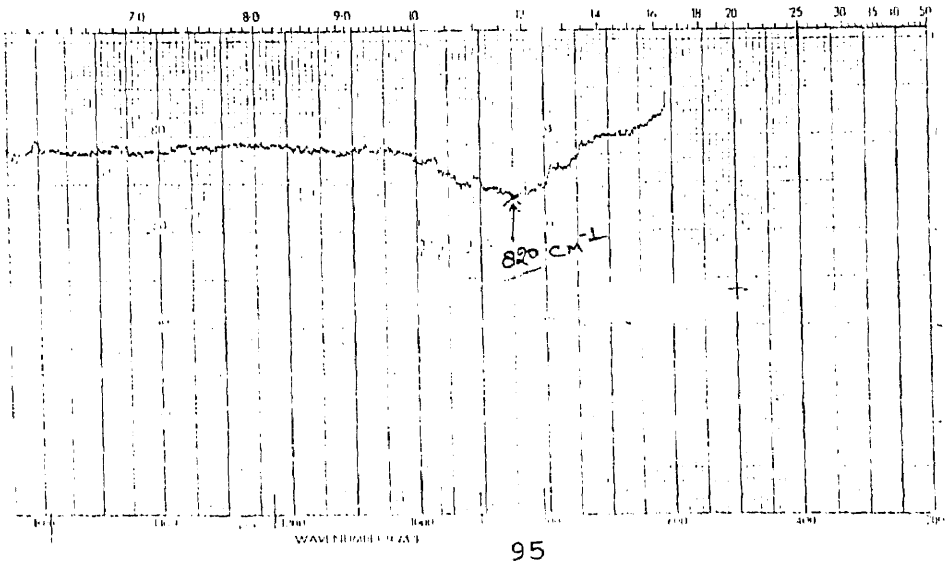

Fig. 7.15

SAMPLE #	CAPACITANCE (nF)	DIELECTRIC CONSTANT
R35S6	8.4	5.9
R41S2C2	4.75	6.1
R41S1	4.6	5.8

TABLE 7.1 CAPACITANCE OF DIELECTRIC CONSTANT OF MIS AT 1 KHz

VIII CONCLUSIONS AND FUTURE REMARKS

8.1.0 CONCLUSIONS:

Sputtered Silicon Nitride films were studied using optical transmission and conductivity measurements. From the analysis of the results, it was concluded that low conductivity films of Si_3N_4 can be successfully prepared by direct sputtering of Silicon Nitride target. Various conclusions drawn from this study are summarized as follows.

(i) Low conductivity stoichiometric (or near stoichiometric) Silicon Nitride films can not be prepared in only Argon plasma and Nitrogen is essential.

(ii) All the samples from the same run did not exhibit homogeniety in the film characteristics.

(iii) Resonable deposition rates can be obtained even with low RF powers, but as the deposition time increases, deposition rate suffers irrespective of the power applied.

(iv) No unique value of dielectric constant is observed and is found to increase with film thickness.

(v) IR results lead to the conclusion that sputtering parameters, except the carrier gas have little effect on optical absorption. Incorporation of impurities like Hydrogen and Oxygen were unavoidable.

(vi) Lower Si/N ratio should be maintained in order to deposit high resistivity films. Lower the ratio, higher will be resistivity.

Sputtered amorphous hydrogenated Germanium films were also prepared and studied. It was proved that thus passivated detectors had improved performances. Results indicate a promising future for this method of passivation.

8.2.0 SUGGESTIONS FOR FUTURE WORK:

This section provides the direction in which this research should advance in order to get better results. These remarks are based upon the results of this research, experience and intuition of the author. Si_3N_4 deposition should be carried out only in Nitrogen or N_2 (90 %)-Ar (10 %) mixture in order to get high resistivity films. Target should be presputtered for atleast 30 minutes prior to deposition in order to get reproducible films. Vacuum chamber should be kept at relatively higher temperatures while not in use, so as to avoid any moisture absorption. Hot water should be used for target cooling between the runs and cold water should be used during the run so that it may help in avoiding moisture absorption in the target. Residual Gas Analyser should be used to determine the composition of sputtering environment during the deposition

run.

Effect of temperature on conductivity should be studied. Instrumentation facilities should be improved. Availability of Ellipsometry and C-V plotter may prove crucial to the furter advancement of this project. Attempts should be made to calculate the surface states which could be done from C-V results. Further attempts should be made to evaluate the composition of the films.

Hall-effect measurements should be done in order to evaluate the a-Ge films. Substrate temperature should be accurately measured and it may yield some important conclusions regarding the growth behavior of the films.

APPENDIX A

DECONTAMINATION PROCEDURE FOR THE MRC 8800 SPUTTERING SYSTEM

The MRC 8800 Sputtering system in Drexler Microelectronics Laboratories at NJIT was used for sputtering of Cadmium Telluride in an atmosphere of Mercury for fabricating Mercury Cadmium Telluride (MCT) heterojunctions for the last eight years. Since the object of this research was changed to passivation of Optoelectronic devices rather than the development of MCT heterojunctions, it was of prime importance to remove even the smallest traces of Mercury from the chamber. The main purpose of cleaning the system was to get rid of the smallest concentration of Mercury. It was a rather difficult task to remove all Mercury traces from the chamber. After a lot of discussions with chemists in the Chemistry Department at NJIT and with those involved in such matters, the following procedure was adopted.

At the outset, the sputtering system was vacuumed with the vacuum cleaner available in the laboratory. It was difficult to remove Mercury from the tiny grooves and regions where the vacuum cleaner hose could not reach. For this purpose, another vacuum cleaning system was designed

and used. The system is shown in the schematic (Figure A1).

The triode box (plasma confinement box) was removed from the vacuum chamber. After dismentalling the triode box, it was cleaned with trichloroethylene (TCL), and then delicately cleaned with fine sand paper. After reassembling, it was again cleaned with TCL and then heated with a heat gun so as to evaporate any TCL, if present. This confinement box consists of four sections. Care should be taken that each of these four sections is electrically isolated.

The filament box and the water lines (for cooling the filament boxes) inside the vacuum chamber were removed. In order to remove the filament box, first the water lines were disconnected from the filament box and then two screws were removed with which the filament box was held in position. Due to glass insulators present behind each of these boxes, careful attention was required during their removal. Figure A2 illustrates the arrangement of water lines and the filament boxes. The water lines enter the vacuum chamber through the base plate. Looking on to the base plate from underneath, these two water lines are seen passing through a flange and are connected to two black poly flow TYGON tubings. This is illustrated in figure A3. After disconnecting these two TYGON tubings, it was possible to pull out the water lines from inside the

chamber.

All water and electrical connections to the anode were disconnected. The anode is held in position by two small screws which are attached to the levers on the hydraulic cylinder under the base plate. The hydraulic cylinder is used to raise or lower the anode. After removing these two screws, the anode was carefully removed from the main chamber. Disassembling of anode is discussed later.

Intervac chamber was disconnected from the main chamber by removing four hex-head screws on the flange which connects the two chambers. This disconnected intervac chamber was balanced on wooden blocks.

All the blank flanges as well as the accessories provided on the vacuum chamber, like vent valve, ionization gauge etc. were removed. The Mercury bottle was removed and placed safely.

The lower half of the vacuum chamber, resting on the base plate, was removed with the help of three hex-head screws inside the chamber. Water lines and electrical connections for both filament feed throughs were removed before the removal of the lower half of the vacuum chamber.

Each and every part of the vacuum station was cleaned with NOXON several times until it started shining. Proper care was taken in cleaning the o-ring grooves with

NOXON. It was ensured that NOXON was never applied on the metal surfaces for any longer duration of time in order to protect the metal surfaces from absorbing NOXON. A small quantity of NOXON was spread on a rag and then metal surface was polished vigorously. Every metal surface on the chamber was cleaned in this manner several times. Finally it was cleaned with TCL several times. The o-rings at the base plate were replaced.

The system was reassembled after all cleaning was finished. All the ports were blanked off except one for venting. At this stage, vacuum chamber was completely stripped of all accessories that is anode, filament box, water lines and intervac chamber. These ports were blanked off using blank flanges. At this stage, vacuum chamber basically comprised of its stainless steel envelope, turret and venting valve. The anode assembly was disassembled to check for any bad parts and for cleaning, as described below. After removing the anode assembly from the chamber, the metal housing for the anode collar in the exterior of the chamber remained. This housing has two garlock seals, two o-rings and a nozzle that connects the differential pumping line from mechanical pump to the anode (for evacuating the anode). It is a two piece structure on which the hydraulic cylinder mentioned above is mounted. Garlock seals are present on the two extreme ends of this housing.

In order to disassemble , first the differential pumping line was disconnected and then the ten hex head screws were removed. Main anode disassembling was performed according to the procedure listed in the lab manual.

Sputtering system is equipped with the rotational turret having four targets. This target assembly is a metallic cubic structure. Targets are fixed on four faces of the cube and on other two faces are the shafts which hold this cubic structure in position. One shaft is connected between the cube on one side and the wall of the chamber on the other (S2 in Figure A4). The other shaft is fixed on the cube on one side and the other side of this shaft (S1 in Figure A4) is fixed to the turret feed through. S1 is the bigger and hollow circular shaft where as S2 is relatively smaller in diameter (than S1) and solid circular shaft. Assembly is illustrated in schematic shown in Figure A4.

Shaft S1 carries the water lines for target cooling. These water lines were designed so as to carry RF voltage too. Water goes to the target # 1 through the "Water In" on the tuning box, gets circulated to targets 2, 3 & 4 and then comes out through "Water Out". To replace the target, it is necessary to reach into the cube. For this purpose, the biggest flange on the chamber was removed, which then disconnected S2 from the chamber wall.

Now S2 needed to be disconnected from the cube. It was done by removing eight hex head screws from the cube which released S2 , from the assembly, along with the face of the cube on which it was welded. It was possible to reach inside the cube and thus remove the target (with the backing plate) by removing the center bolt (see Figure A5) with which it was secured in position. This bolt is not visible from outside and one has to reach it from inside the cube. It is in the center of the target backing plate. One has to be extremely careful while removing this screw otherwise one might drop the target or crack the pyrex insulator, a part of the target assembly. There were two o-rings on the backing plate , visible only after removing the target. Grooves for these o-rings are not on the backing plate but on the structure protruding from the cube face. A vacuum leak which was observed in the top half of the chamber was due to bad o-rings mentioned above. To remove the entire target unit from the cube, the eight outermost hex head screws were removed from inside the cube, which then released the entire target unit from the cube. It comprised of a stainless steel ring (3/4" thick), pyrex insulator ring and an arrangement for target cooling. The assembly is very much similar to the main anode internal assembly. There are two gaskets, one for each side of pyrex and four o-rings in one target assembly. After

cleaning, all the seals and damaged parts were replaced and the unit was reassembled. Water lines are very critical and were disconnected before the entire assembly was disconnected from cube. While reassembling, one must ensure that the water lines coincide with the opening on the backing plate and are free from any water leaks. Same procedure was repeated for the rest of the targets.

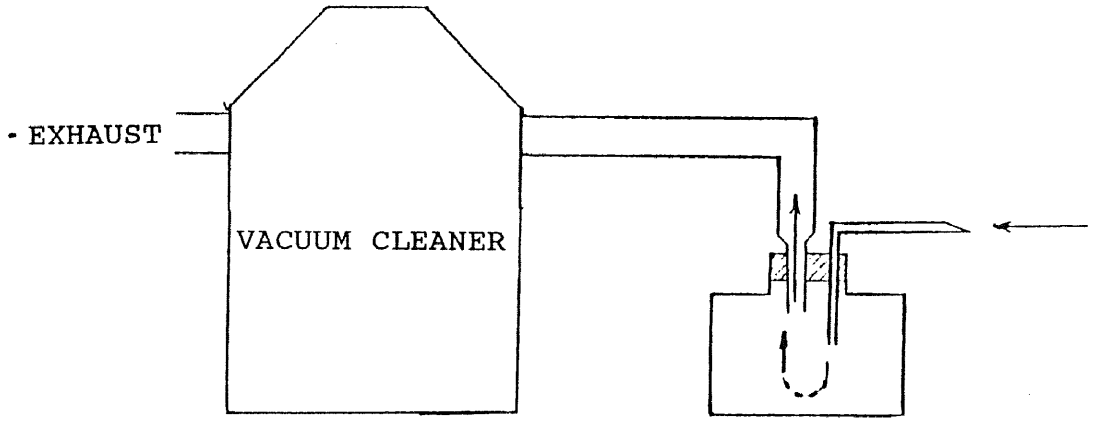

Fig. A1 APPARATUS USED FOR VACUUM CLEANING OF THE SPUTTERING SYSTEM.

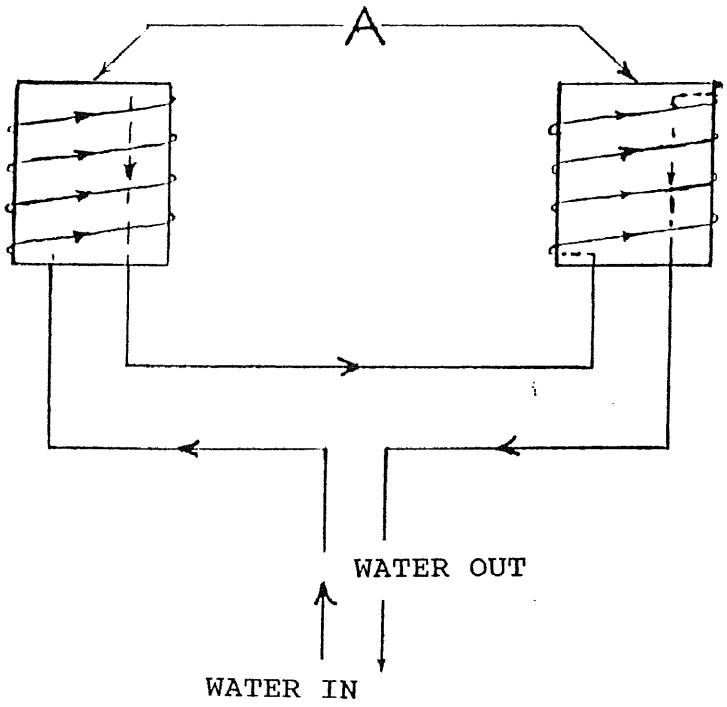

Fig. A2 : FILAMENT BOX WATER LINES
A: FILAMENT BOXES

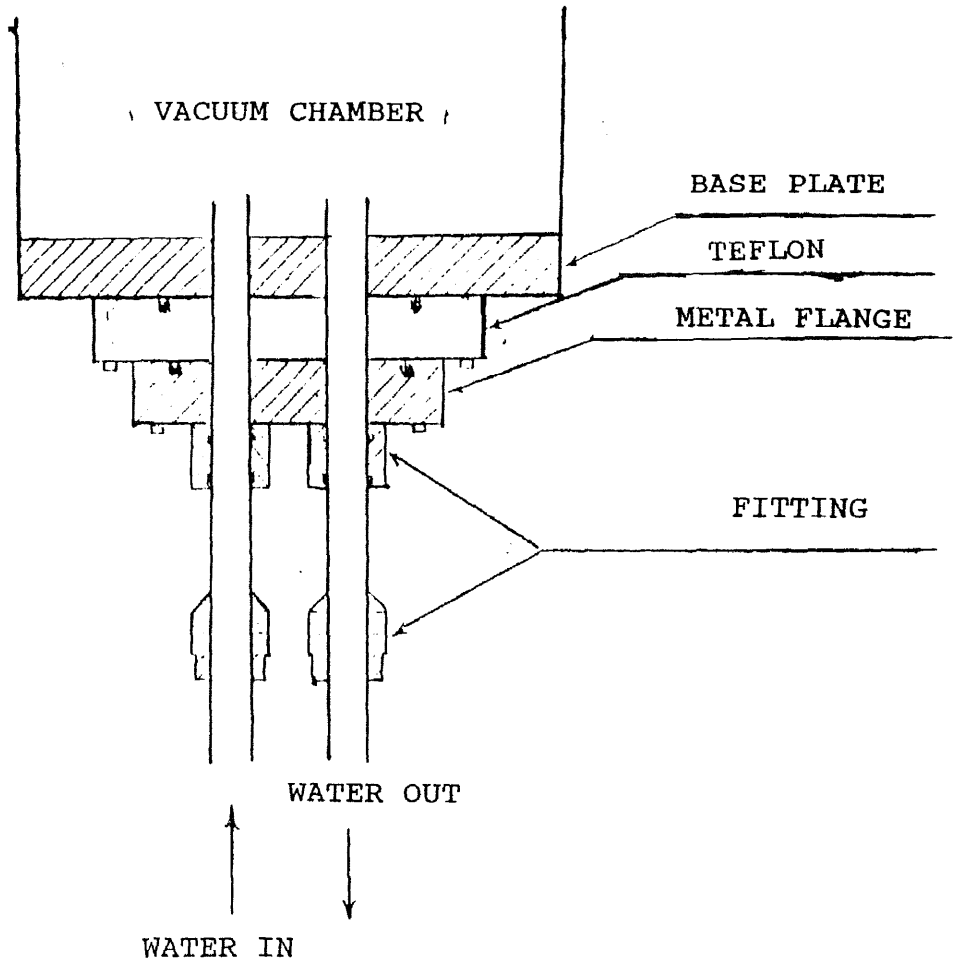

Fig. A3 COOLING WATER FEED THROUGH.

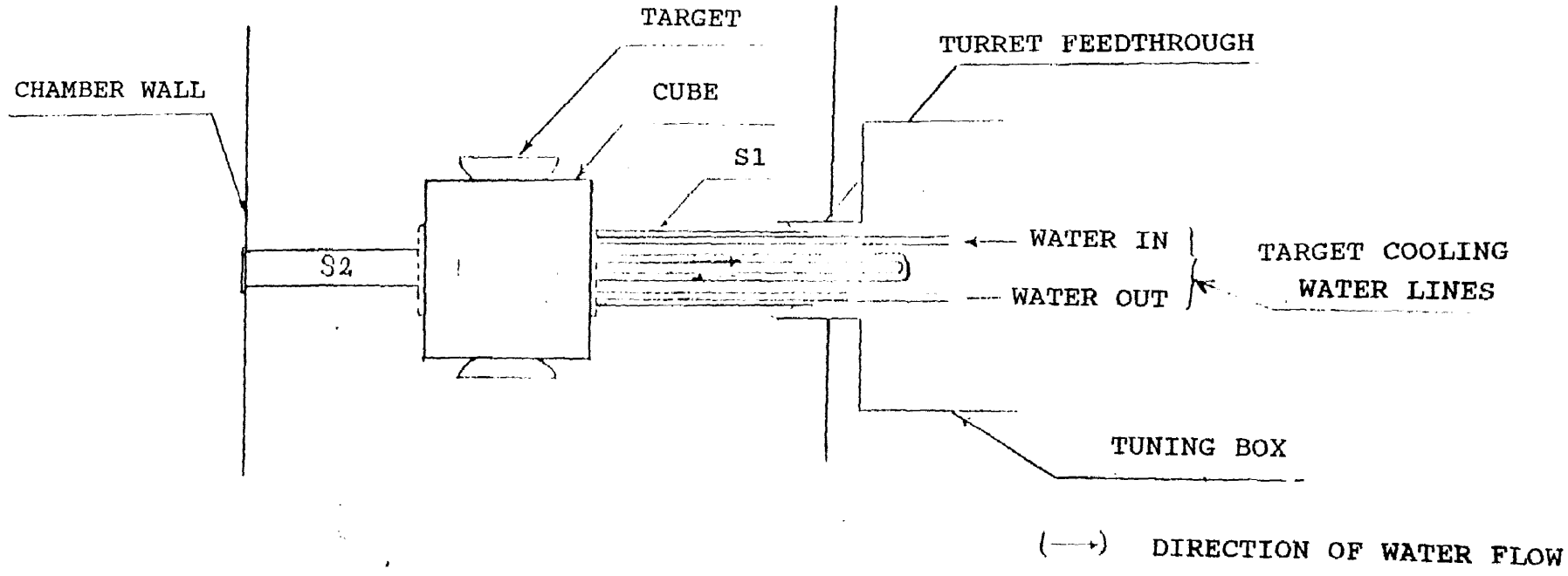

Fig. A4 TURRET HEAD AND TARGET COOLING SYSTEM.

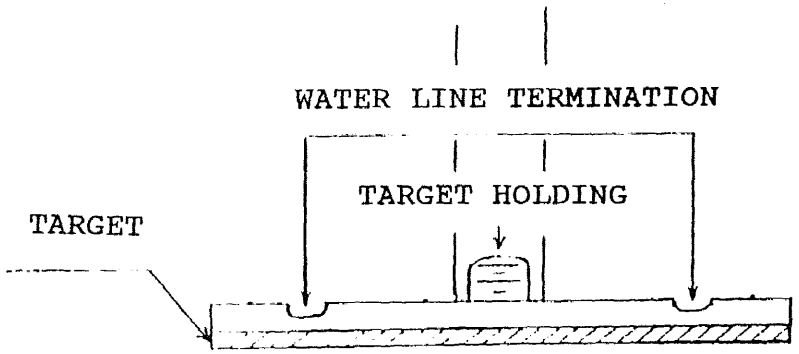

Fig. A5 : CROSS SECTION OF BACKING PLATE AND TARGET.

APPENDIX B

LEAK DETECTION

The system was taken apart to detect the location of the vacuum leak, as explained in the preceeding section. Before it was taken apart, all possibilities of leaks were eliminated, like blanking off all the ports, changing the o-rings etc. But after doing all this, pressure never went down. When the chamber was being roughed, a hissing noise of a leak was heard. All possible locations were checked. All possible methods including soap-water, stethoscope, Freon etc. were tried, but the actual place of the leak could not be determined. This was a major leak, so it was finally decided to take the whole chamber apart and then after cleaning, while reassembling check for the leak section by section. Another important factor towards this decision was that even when it was tried to rough only the lower portion of the chamber, it couldn't be roughed and the hissing noise was still present. It was ensured that atleast one major leak was present in the lower part of the chamber.

After cleaning each and every part, all the o-rings were replaced while reassembling the system. Upto this stage, intervac chamber was not connected to the main

chamber. The following course was selected to locate the leak.

(1) All the main ports were blanked on the lower half of the chamber, except one on which the venting valve was connected for venting the chamber. This means that the flange connections for the intervac chamber, openings in the base plate for the filament box water lines and for the anode were also blanked. Now roughing was attempted on the lower part of the chamber (for about an hour). No improvement in the vacuum conditions were observed. The thermocouple gauge indicated about 1000 microns. There was still a hissing noise of the leak, from the chamber. The pump was turned off after closing the roughing valve and then all the power to the system was turned off, eliminating all possible sources of noise in the laboratory. Now it was tried to investigate where this noise was coming from but the cause could not be determined.

(2) Soap bubbles, stethoscope, Freon etc. were used but the desired results were not achieved.

(3) The High vac/roughing valve opening in the chamber, on the the base plate was blanked and roughed so as to ensure that there was no leak through the roughing valve or high vac valve. Pressure went below 100 microns. It ensured that there was no leak here.

(4) Now even the venting valve was replaced with a blank flange and the lower part of the chamber was roughed. There was no improvement. It ensured that there wasn't any leak through venting valve. It was replaced again.

(5) It was suggested that welding on the walls might have been damaged . It was checked but found no damage.

(6) Now the concentration was on the three small opening in the chamber. One was in the wall of the lower part of the chamber and two of them were in the base plate, behind the anode. All these openings were blanked off in the past. Two of these were easily accessible but one was very difficult to reach. This one was behind the cryopump and from outside, it was never seen what was connected there, simply because it was not visible at all. Since the other two were blanked, it was thought that this one was also blanked, but it was not so. It was found that a pressure switch was connected there. By this time, this was the only part that hadn't been replaced or checked. It was then decided to replace this switch by a blanking plug. After blanking this, the lower half of the chamber was roughed. The pressure went below 100 microns. So this pressure switch was contributing a major role in the massive leak.

At this stage except the venting valve, all other ports were blanked. The anode collar housing was reinstalled and the lower half of the chamber was checked

again for leaks. Again a leak was observed. The leak must have come from this housing, and therefore it was removed. It was agreed to rough the housing with the anode, through the differential pumping line, outside the chamber. It was observed that the leak persisted as the pressure did not go down. Now the garlock seal was removed from the housing and it was found that the o-ring was not damaged. The o-ring was replaced again and the housing was roughed with the anode in it. Now the leak was eliminated. Then, anode was placed in the chamber and the lower half was roughed again. Still the Intervac and the water lines for filament boxes were not connected. Now after roughing the lower half for half an hour, the pressure went down, Thus till this stage everything was satisfactory. Now the intervac chamber was connected, the lower half was roughed and the vacuum was found to be satisfactory. The next step was to connect the water lines for filament boxes and the filament boxes themselves. Again after connecting these, the vacuum was checked and found to be satisfactory. Entire chamber was roughed. But some leaks were still present. Again, only the lower half of the chamber was roughed and was found to be free of leaks. Thus all possibilities of leaks were eliminated in the lower half of the chamber. Now the cause of leak in the top half of the chamber was to be detected. It was thought that it must be from one of the targets

since all of them had been taken apart. Once again all the targets were removed and checked for poor o-rings and cracked pyrex ring. After reassembling all the targets, an attempt was made to rough the chamber and the leak was found to be eliminated. This entire leak detection and decontamination of the vacuum station took almost six months.

APPENDIX C

INFRARED TRANSMISSON MEASUREMENT

I. Switch the instrument on. Scan the instrument to 4000^{-1} using Fast Forward/Reverse Control and allw ot to warm up for 30 minutes.

II. Position the chart so that the chart grid is synchronized with the wave number scale setting and ensure that the chart drive is enganged.

III. Select medium scan mode and 'N' slit size for thin substrates (7 mils) and slow scan mode and '7' slit size for thick substrates (15 mils).

IV. Place the reference and the sample (whose IR is to be taken) substrates in the reference and the sample beams respectively.

V. Check and adjust BALANCE once everyday as follows:

(i) Place a strip of opaque material blocking both beams simultaneously. Manually move the pen carriage slowly to the middle of the transmission scale. Pen should either remain stationary or drift slowly upscale indicating that the instrument is properly balanced.

(ii) If the instrument is out of balance, adjust the BALANCE control on the side of the instrument until the proper balance is established.

VI. Adjust the GAIN control once every day as follows:

(i) Turn the GAIN control to minimum.

(ii) Set the 100 % control so that the pen indicates 90 % transmittance.

(iii) Insert finger in the sample beam to partially block it until the pen is deflected 2 to 3 %. Allow the pen to settle and then rapidly remove the finger. Pen should return to a constant reading of approximately 90 % transmittance.

(iv) Introduce a finger in the reference beam to partially block it until the pen is deflected 2 to 3 %. Allow it to settle and then rapidly remove the finger. The pen will return to a constant reading that may differ from the level observed in step (iii), the gain setting should be adjusted to reduce this difference to not more than 1/4 % transmittance.

VII. Before transmittance measurement on each sample, adjust the 100 % control until the pen reads 100 % transmittance.

VIII. Run 100 % transmittance scan with the reference samples in both the beams.

IX. Run 0 % transmittance scan with the reference sample in the reference beam and blocking the sample beamwith the sample holder.

X. Run the transmittance scan for the unknown sample by

placing the reference and the unknown samples in their corrosponding beams.

REFERENCES

1. Grove, A. S., "Physics and Technology of Semiconductor Devices", John Wiley and Sons, New York (1967).

2. Nicollian, E. H., J. Vac. Sci. and Tech., 8, S39 (1971).

3. Snow, E. H. and Deal, B. E., Trans. Met. Soc. AIME, 242, 521 (1968).

4. Szedon, J.R. and Handy, R. M., J. Vac. Sci. and Tech., 6, 1 (1969).

5. Swaroop, B., J. Electrochem. Soc., 118, 913 (1971).

6. DiGiacomo, G., J. Electrochem. Soc., 121, 419 (1974).

7. Pink, F. X. and Lyn, V., Electrochem. Tech., 6, 258 (1968).

8. Smith, J.N., Thomos, S. and Ritchie, K., J. Electrochem. Soc., 121, 827 (1974).

9. Sato, J., Ban, Y. and Maeda, K., 9th Ann. Proc. Rel. Phys., pp. 96-106 (1971).

10. Arai, E. and Terunuma, Y., J. Electrochem. Soc., 121, 676 (1974).

11. Daghir, K. S., Abstract 268, p. 666, The Electrochem. Soc. Extended Abstracts, Fall meeting, Miami Beach, Florida, Oct. 8-13, 1972.

12. Castagne, R.,Hesto, P. and Vapaille A., Thin Solid

Films, 17, 253 (1973).

13. Hoffman, R. W., in "Measurement Techniques for Thin Films", Schwartz, B. and Schwartz, N., editors, pp. 312-333, The Electrochem. Soc. Softbound Symposium Series, New York (1967).

14. Scheuerman, R. J., in "Thin Film Dielectrics", Vranty, F., Editor, pp. 561-576, The Electrochem. Soc. Softbound Symposium Series, New York (1969).

15. Schaible, P. M. and Glang, R., in "Thin Film Dielectrics", Vranty, F., Editor, pp. 577-594, The Electrochem. Soc. Softbound Symposium Series, New York (1969).

16. Swaroop, B., ibid., pp. 407-431 (1969).

17. Pliskin, W. A., Davidse, P. H., Lehman, H. S. and Maissel, L. I., IBM J. Res. Develop., 11, 461 (1967).

18. Goldsmith, N. and Kern, W., RCA Rev., 28, 153 (1967).

19. Gregor, L. V., Proc. IEEE, 59, 1390 (1971).

20. Attala, M. M., Tannenbaum, E. and Scheibner, E. J., Bell Sys. Tech. J., 38, 749 (1959).

21. Sze, S. M., J. Appl. Phys., 38, 2951 (1967).

22. Hu, S. M. and Gregor, L. V., J. Electrochem. Soc., 38, 831 (1967).

23. Grieco, M. J., Worthing, F. L. and Schwartz, B., J. Electrochem. Soc., 115, 521 (1968).

24. Brown, G. A., Robinette, W. C. and Carlson, H. G., J.

Electrochem. Soc., 115, 948 (1968).

25. Gregor, L. V., IBM Technical Report, (1968).

26. Vossen, J. L., J. Vac. Sci. and Tech., 8, 751 (1972).

27. Doo, V. Y., Nichols, D. R. and Silvey, G. A., J. Electrochem. Soc., 113, 1279 (1966).

28. Simmons, J. G., Electronic Conduction Through Thin Insulating Films, in Handbook of Thin Film Technology, Maissel and Glang, Editor, (1980).

29. Hass, J. G., Am. Ceram. Soc., 33, 353 (1958).

30. Ritter, E., Opt. Acta., 9, 197 (1962).

31. Brady, G. W., J. Phys. Chem., 63, 1119 (1959).

32. Simmons, G. J., Phys. Rev., 155, 657 (1967).

33. Frenkel, J., Phys. Rev., 54, 647 (1938).

34. Maes, H. E. et al., Proc. of Symp. on Silicon Nitride Insulating Thin Films, Kapoor, V. J. and Stein, H. J., Editor, Vol. 83-8, 177 (1985).

35. Hanson, W. L., Hallu, E. and Hubbard, S. G., Trans, IEEE (Nuclear Science), NS-27 (1980).

36. Roop, R. M. and Saltich, J. L., International Electron Devices Meeting, Washington D.C. (Dec. 4-5-6), pp. 456-459 (1978).

37. Taft, E. A., J. Electrochem. Soc., 122, 1341 (1971).

38. Mogab, C. J., Petroff, P. M. and Sheng, T. T., J. Electrochem. Soc., 122, 815 (1975).

39. Kominiak, G. J., J. Electrochem. Soc., 122, 1271

(1975).

40. Mogab, C. J. and Lugujjo, E., J. Appl, Phys., 47, 1302 (1976).

41. Cornely, R. H., Personal Communications.

42. Luongo, J. P., Appl. Spectroscopy, 38, 2, 196 (1984).

43. Rigo, S., Amsel, G. and Croset, M., J. Appl. Phys., 47, 1302 (1976).

44. Sze, S. M., "Physics of Semiconductor Devices", John Wiley & Sons, New York (1981).

45. Cho, Masters's Thesis on Sputtered a-Ge Films: to be published.

46. Deal, B. E., Fleming, P. J. and Castro, P. L., J. Electrochem. Soc., 115, 300 (1968).

47. Swaroop, B. and Schaffer, P. S., J. Appl. Phys. (U. K.), 3, 803 (1970).